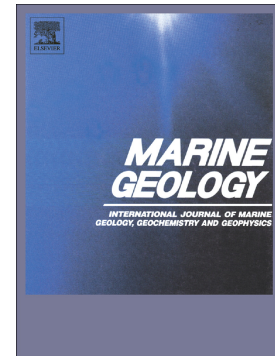


Accepted Manuscript

Seismic geomorphology of submarine channel-belt complexes in the Pliocene of the Levant Basin, offshore central Israel

Yakufu Niyazi, Ovie Emmanuel Eruteya, Kamal'deen Olakunle Omosanya, Dicky Harishidayat, Ståle Emil Johansen, Nicolas David Waldmann



PII: S0025-3227(17)30517-0
DOI: doi:[10.1016/j.margeo.2018.05.007](https://doi.org/10.1016/j.margeo.2018.05.007)
Reference: MARGO 5797
To appear in: *Marine Geology*
Received date: 22 October 2017
Revised date: 8 April 2018
Accepted date: 23 May 2018

Please cite this article as: Yakufu Niyazi, Ovie Emmanuel Eruteya, Kamal'deen Olakunle Omosanya, Dicky Harishidayat, Ståle Emil Johansen, Nicolas David Waldmann , Seismic geomorphology of submarine channel-belt complexes in the Pliocene of the Levant Basin, offshore central Israel. The address for the corresponding author was captured as affiliation for all authors. Please check if appropriate. Margo(2017), doi:[10.1016/j.margeo.2018.05.007](https://doi.org/10.1016/j.margeo.2018.05.007)

This is a PDF file of an unedited manuscript that has been accepted for publication. As a service to our customers we are providing this early version of the manuscript. The manuscript will undergo copyediting, typesetting, and review of the resulting proof before it is published in its final form. Please note that during the production process errors may be discovered which could affect the content, and all legal disclaimers that apply to the journal pertain.

Seismic geomorphology of submarine channel-belt complexes in the Pliocene of the Levant Basin, offshore central Israel.

Yakufu Niyazi^{1,*}, Ovie Emmanuel Eruteya^{1,2}, Kamal'deen Olakunle Omosanya³, Dicky Harishidayat³, Ståle Emil Johansen³, Nicolas David Waldmann¹

¹Dr. Moses Straus Department of Marine Geosciences, Leon H. Charney School of Marine Sciences, University of Haifa, Haifa 3498838, Israel

²Department of Earth Sciences, University of Geneva, 1205 Geneva, Switzerland

³Department of Geoscience and Petroleum, Norwegian University of Science and Technology, 7031 Trondheim, Norway

* Corresponding Author: Yakufu Niyazi, email: yniyazi@campus.haifa.ac.il

Abstract

In this study, analyses of a high-resolution, three-dimensional seismic reflection dataset and well-log data were combined to characterise a distinct Pliocene interval in the Levant Basin offshore central Israel. This succession is characterised by moderate to high-amplitude, discontinuous to continuous seismic reflections between a mass transport deposit above and an undeformed basin series below. The studied interval contains two separate channelised subunits. Morphologically, the channels trend in a north to northwest direction, are incised <50 m, are ~50 m to 350 m wide and increase in number from base to top. A vertical variation in channel morphology style and stratigraphic organization is identified. The lower part of each subunit is dominated by coarser grained, narrow V-shaped channels (average width <120 m and low sinuosity, <1.06). In contrast, the upper part of each subunit is predominantly fine-grained and U-shaped with relatively wide channels (average width >230 m and higher sinuosity, >1.1). The mechanisms that control the interplay between sedimentary processes and channel evolution show a cyclic pattern. Due to the cyclic occurrence of different channel types and the estimated age of the studied interval, formation and evolutionary processes of the submarine channels in the study area are likely to be controlled by relative sea level fluctuations and increased Nile River sediment supply, which is associated with rapid uplift of the Ethiopian plateau and increased African Monsoon rainfall during the Pliocene.

Keywords: Submarine channels; seismic geomorphology; sea level fluctuations; sediment supply; African Monsoon; Levant Basin

1. Introduction

Submarine channels are pervasive geomorphic features documented on both the modern-day seafloor and in the geological record buried intervals within marine settings (Feng, 2000; Posamentier et al., 2000, 2007; Posamentier, 2001; Miall, 2002; Carter, 2003; Posamentier and Kolla, 2003; Saller et al., 2004; Samorn, 2006; Wood, 2007; Gamboa et al., 2012; Gamboa and Alves, 2015; Harishidayat et al., 2015; Qin et al., 2016). They represent major conduits for transporting sediments from the shelf and upper slope into the deep basin (Piper and Normark, 2001; Babonneau et al., 2002), and have been described in detail within the submarine fans that are associated with major river systems such as the Niger (Deptuck et al., 2003; Adeogba et al., 2005; Heiniö and Davies, 2007), Mississippi (Pickering et al., 1986; Posamentier, 2003), Amazon (Damuth et al., 1983; Flood and Damuth, 1987), and Bengal (Hübscher et al., 1997; Schwenk et al., 2003) rivers.

Submarine channels have been the foci of several studies in the last decade as they can serve as prime targets for petroleum exploration (Mayall et al., 2006, 2010; Weimer et al., 2007; Di Celma et al., 2010), and may have significant implications for geohazard prediction and prevention (Bruschi et al., 2006; Thomas et al., 2010; Carter et al., 2014). Additionally, they can also hold significant sedimentological and climatic information on the controlling mechanisms behind their formation (Bouma, 2001; Brenchley et al., 2006; Zühlsdorff et al., 2007; among others). As a result, much work has focused on the depositional processes, internal architecture, and morphological evolution of submarine channels (Posamentier and Kolla, 2003; Babonneau et al., 2010; Covault et al., 2014; Li and Gong, 2016; Sylvester and Covault, 2016; Hansen et al., 2017). Past studies have mostly focused on the understanding of initiation, geomorphological characteristics, and development of submarine channels and are mostly based on outcrops, recent fan systems, and 2-D reflection seismic studies (Bouma, 1962; Mutti and Ricci Lucchi, 1972; Walker, 1978; Posamentier et al., 1991; Mutti and Normark, 1991). This has been due to the paucity of high-resolution deep subsurface geophysical datasets, which are recently becoming available to academia as hydrocarbon exploration transits into deep and ultra-deep waters (Pirmez et al., 2000; and others).

This study presents seismic geomorphological analysis of a channelised interval developed during the Pliocene in the deep Levant Basin, offshore central Israel (Fig. 1). Previous studies in the region only focused on recent and Holocene submarine channels and

their interaction with subsurface salt tectonics (e.g., Folkman and Mart, 2008; Clark and Cartwright, 2009; Gvirtzman et al., 2015; Zucker et al., 2017). The nature and evolutionary history of deeper channelised units remain poorly constrained. A high resolution, 3-D seismic reflection data was employed to: (1) characterize and classify submarine channels that were developed in the Pliocene interval of the Levant Basin, (2) investigate the influences of salt tectonics on channel evolution, (3) demonstrate their spatio-temporal distribution and stratigraphic organization, and (4) suggest possible controlling mechanisms on their initiation and evolution. The findings from this study have important implications for better understanding the geomorphological characteristics and development of submarine channels in deep marine settings as well as possible interactions with sub-channel, salt-related deformations. At a local scale, we have provided new insights into the environmental setting and geological mechanisms behind the formation and evolution of submarine channels in the Levant Basin during the Pliocene.

2. Geological settings

The Levant Basin is in the SE part of the East Mediterranean (Fig. 1a). A carbonate platform developed in the basin that started with post-rift activity during the Triassic and continued until the Late Cretaceous, when it became intermittently drowned and pelagic sedimentation dominated (Druckman et al., 1995; Garfunkel, 1998; Gardosh et al., 2008a). During the Oligo-Miocene, several submarine canyons (e.g., el-Arish, Afiq and Ashdod) incised the shelf and transported terrestrial siliciclastic deposits to the deep basin (Druckman et al., 1995; Gardosh et al., 2008b). The more recent geological history of the Levant Basin is dominated by the Messinian Salinity Crisis (MSC) of 5.9-5.3 Ma (Hsü, et al., 1978; Roveri et al., 2014). The MSC resulted in desiccation of the Mediterranean Sea and the deposition of a 1.5-2 km thick unit of alternating halite, gypsum, and clastic sediments (Bertoni and Cartwright, 2005; Feng et al., 2016; Fig. 2). A prominent high-amplitude reflection with distinct topography at the top of the evaporites is well recognised on seismic profiles across large parts of the Mediterranean Sea (Lofi et al., 2011; Roveri et al., 2014), which is interpreted as the top of the Messinian Evaporites, and hence serves as a regional chronological marker in this study (Fig. 2).

The Plio-Pleistocene geological evolution of Levant Basin is largely controlled by the progradation of Nile-driven sediments and salt tectonics. Following the end of the Messinian Salinity Crisis (5.33 Ma), restoration of open marine conditions in the Mediterranean was accompanied by formation of the modern-scale Nile Delta (Said, 1981). Although a deep-water

turbidite sandy fan (identified as the Yafo Member), sourced from the Levant margin during the early Pliocene, was developed over areas previously occupied by Oligo-Miocene submarine canyons, it was immediately buried by Nile driven sediments (Frey Martinez et al., 2005).

The Nile is one of the longest rivers on Earth (>6500 km) and is fed by summer monsoon rains over the East African highlands (Fig. 1a). The Nile delta has a width and length of more than 600 km and 300 km, respectively. Thus, forming the largest and thickest sedimentary unit characterised by one of the highest accumulation rates in the world (Reading and Richards, 1994; Loncke et al., 2002; Ducassou et al., 2009; Gvirtzman et al., 2015). From the beginning of the Pliocene, the Nile Delta was subjected to increased sedimentation derived from augmentation in the monsoonal rains over the tropical East Africa highlands (deMenocal, 1995, Larrasoña et al., 2003). Transport of the Nile-driven sediments along the Levant coastline and the shelf by counter-clockwise currents promoted deposition of clay-rich marls in the deeper areas of the basin, and peak sediment supply to the Levant Basin was reached during mid-late Pliocene (Zviely et al., 2007; Macgregor, 2011). This increase in sediment supply was aided by submarine channels, which developed during the Pliocene lowstand (Aal et al., 2000; Kellner et al., 2009).

The combination of gravitational collapse on the slope and subsequent basinward spreading of the Nile cone over the ductile Messinian evaporites further deformed the post-Messinian sedimentary overburden at the end of the Pliocene (Tibor et al., 1992; Frey Martinez et al., 2005; Gvirtzman et al., 2013; Fig. 2). This situation, in turn promoted slope instability and successive episodes of submarine mass wasting (Cartwright and Jackson, 2008; Katz et al., 2015; Eruteya et al., 2016; Fig. 2). The Quaternary section of the Levant Basin is characterised by long and sinuous submarine channels, which are ubiquitous on the present-day seafloor and influenced strongly by subsurface salt tectonics (e.g., Loncke et al. 2006; Clark and Cartwright 2009; Ducassou et al. 2013; Gvirtzman et al. 2015; Zucker et al., 2017; Fig. 1b and 1c).

3. Database and Approach

The seismic datasets used in this study include 2-D and 3-D seismic data. The A 2-D time-migrated multi-channel seismic survey was acquired in 2001 by TGS-Nopec and served as the background for geophysical interpretation. This survey was acquired with the following parameters: a 5,000 in³ airgun array placed 5±1 m below the sea surface, 25 m shot interval, a 7.2 km long digital Hydrosience streamer with 567 channels and a group interval of 12.5 m. The record length reached 9 seconds two-way time (TWT), with a sampling interval of 2 ms and a fold of 144. Standard industrial processing was conducted by TGS-Nopec. The 3-D

dataset comprises a pre-stack depth migrated (PSDM), high resolution, three-dimensional (3-D) seismic reflection survey (known as the Sarah-Myra survey). The 3-D dataset covers an area of about 1350 km² in water depths of 1100-1500 m, about 50 km offshore central Israel (Fig. 1b), and was acquired using 10 streamers, each 6 km long, with a 12.5 m group interval. For the 3-D seismic survey, the separation between the streamers was 100 m and spatial resolution was 25×12.5×5 m (x-y-z). The seismic data are zero-phased at the seabed reflection and displayed using Society of Exploration Geophysicists (SEG) normal polarity (Brown, 2004). Hence, a positive event represents a downward increase in acoustic impedance (red reflection on seismic sections), and a negative event represents a downward decrease in acoustic impedance (blue reflection on seismic sections). The wireline log data was mainly gamma ray log from the Myra-1 wellbore (Fig. 1c).

The classical seismic stratigraphic interpretation technique of Mitchum et al. (1977) was used and the seismic section was classified into four main units based on the observations of this study and the stratigraphic scheme of Eruteya et al. (2015). Identification and mapping of submarine channels was achieved using a seismic geomorphological approach, which include a combination of horizontal depth slices and iso-proportional slices (Fig. 3; sensu Zeng et al., 1998; Zeng, 2001; Posamentier, 2003; Brown, 2004; Kolla et al., 2007). In addition, seismic attributes such as maximum amplitude, RMS (Root Mean Square) amplitude and variance, were extracted along and within the horizons to illuminate and visualize the channels as well as to characterize geological anomalies that are isolated from background features by an amplitude response (Taner, 2001). The RMS amplitude maps are mathematically computed by squaring individual traces over a defined time window. They boost high amplitudes in an interpreted interval, allowing the amplitude reflections related to sands within channels to be discriminated from their associated low amplitude chaotic masses (Brown, 2004; Omosanya and Alves, 2013). Variance is the direct measurement of the dissimilarity of seismic traces. Variance maps convert a volume of continuity into a volume of discontinuity, highlighting structural and stratigraphic boundaries (Brown, 2004; Zervas et al., 2018). On the variance attribute maps, faults represent trace-to-trace variability and were mapped as high variance coefficient features.

The scale, geometries, and stratigraphic organization of submarine channel systems were illustrated on both planform and section views generated from the seismic data. Each resulting map is a composite of several observations from a series of closely-spaced depth slices or iso-proportional slices (2-4 m or 3-5 m thick), which are representative of the styles of submarine channel systems within either the lower or upper halves of each seismic unit (Fig.

3; Miall, 2002; Darmadi et al., 2007). Channels from each part of the interval were examined, considering parameters of meandering morphology and respective channel sizes [channel width (CW) and channel relief (CR); Fig. 2a]. The CW and CR were measured at 500 m intervals along the sinuous channel segment, using seismic profiles perpendicular to the path of the channel axis, at each measurement location (Fig. 3b). Channel sinuosity and length were measured along the main channel axes, while a straight line was measured between the starting and ending points of a single channel, as identified in the 3-D dataset (Fig. 3). Following this step, the resulting parameters were used to evaluate the planform morphology of the channel system at various intervals. In this study, the sinuosity classification of Mueller (1968) was used, where straight, sinuous, and meandering channels have sinuosity indexes (SI) of <1.05 , $1.05-1.5$ and >1.5 , respectively. Channel orientation was determined by measuring the mean azimuth of each channel, which was constrained by the locations at which the channel entered and exited the mapped areas.

4.0. Observations and Interpretation

4.1. Seismic stratigraphy

The Messinian evaporites (SU1 in this study) serve as the lowermost boundary for mapping the Plio-Pleistocene sequence (Figs. 2 and 4a). The main stratigraphic interval of interest in this study lies within the Plio-Pleistocene overburden succession of the Messinian evaporites in the Levant Basin (SU2). The Plio-Pleistocene overburden (SU2) has been divided into four main seismic units: SU-2A, SU-2B, SU-2C, and SU-2D based on differences in the internal seismic reflection configurations (Fig. 4a). Channel like incisions were identified only in units SU-2B and SU-2D (Fig. 4a). To investigate the geomorphological history of the submarine channels in the deeper unit, we focused on the SU-2B unit, which consists of moderate- to high-amplitude, sub-parallel and discontinuous to continuous reflections (Fig. 4a). Unit SU-2B is bounded by horizons A and C (at the bottom and top, respectively; Fig. 4b), and thins towards the east and north (Fig. 2). Incisional troughs within this unit were identified and interpreted as deep-water channels (Figs. 4a and 6), with high-amplitude reflections at their bottoms probably representing relatively coarser channel lag deposits (*sensu* Janocko et al., 2013 and references therein). The low amplitude, uniform conformable horizon B drapes the channel incisions in their lower parts and can be traced with remarkable continuity, subdividing the unit into a lower SU-2B-I and an upper SU-2B-II (Fig. 4). The gamma ray (GR) values in these two subunits show symmetrical cyclic patterns characterised by decreasing (from 40 to 25 API) and increasing (from 25 to 50 API) upward trends, suggesting a coarsening upward

trend in the lower part of each subunit and fining upward trend in the upper part (Fig. 4b). The peaks in GR coincide with boundaries of the subunits (horizons A, B, and C), perhaps pointing to rich clay content at these levels. The subunits have similar thicknesses (~30 m – 110 m) and thin towards the northeast (Fig. 5a and b, respectively). However, some fault-related structures have increased the thickness locally (Fig. 2), indicating a localised depocenter without any significant shifting during these periods.

Interaction between the channels and tectonic structures was also identified (Fig. 6). Several faults detaching from the Messinian evaporites were observed in association with folding of the overlying sediment (Figs. 4a and 6, respectively). Within unit SU-2B, the buried channels provide classic markers for relative timing and classification of faults. For example, sinistral strike-slip faults dissect some channels, but in other locations these channels are not intersected. The channels are instead observed above folds and are usually undeformed by post-depositional tectonics (Fig. 6).

4.2 Stratigraphic organization and geomorphology of the submarine channel belt

The submarine channel incisions observed from the lower parts of subunits are V-shaped in cross section, while channel incisions from the upper parts of subunit are U shaped with wider angle, flat or curved bases (Fig. 7). Based on this observation, submarine channels from different parts of the study unit were mapped using depth slices and iso-proportional slices. Ten distinct V-shaped incised, relatively straight, and shallow channels with an average width of 130 m and an average relief of 23 m were mapped in the lower part of SU-2B-I. An additional twenty-two U-shaped incised relatively sinuous, deeper (average relief of 33 m) and wider (average width of ~200 m) channels were mapped in the upper part of SU-2B-I (Figs. 7 and 8a; Table 1). In the lower part of SU-2B-II, twelve V-shaped incised low sinuous, shallow (average relief of 22 m) and narrow (average width of 120 m) channel incisions were identified. Twenty-Three U-shaped, relatively sinuous, deeper (average relief of 31 m) and wider (average width of 198 m) channel incisions (Figs. 7 and 8b; Table 1) were identified in the upper part of the SU-2B-II sub-unit. These plan- and section-view geomorphological parameters allow the observed submarine channels to be categorised into two main types: Type-1 channels that are V-shaped, relatively straight, and narrow, and Type-2 channels that are U-shaped, relatively sinuous, and wide (Table 1). The lower parts of SU-2B-I and SU-2B-II are dominated by Type-1 channels that have orientations of 15° and 2°, respectively (Fig. 8). The upper parts of SU-2B-I and SU-2B-II have predominantly Type-2 channels with orientations of 4° and 6°, respectively (Fig. 8).

The unique seismic geomorphological features associated with the two channel types are presented in Table 2 (see also Fig. 9). Type-1 channels are infilled with continuous and variable amplitude reflections. They show small (~12 m) downward bending reflections that reveal convex-upward shape filling at the top (Fig. 9a). Additionally, Type-1 channels have no related large levee structures, and in the RMS amplitude extraction map they demonstrate higher values that contrast to the surrounding low amplitude strata (Fig. 10). Type-2 channels have much more complex seismic expressions than those characterising Type 1 channels (Fig. 9). The channels infill comprises of low- to high-amplitude, low-frequency and sub-parallel seismic reflections with vertical aggradation that show either concave-upward geometry or shingled dipping to flat and parallel reflections in the channel fill (Figs. 9). Laterally migrated sinuous channels can be identified in the depth slices in the upper parts of the subunits. They are also displaced by faults, infilling with concave-upward geometry (Fig. 11). Thin and low amplitude reflections onlap the underlying reflections within the sides of isolated Type-2 channels. These low amplitude reflections are interpreted as channel levees (Fig. 9d). On the inner channel bends, Type-2 channels are flanked by high amplitude, shingled reflections that dip towards the last-stage channel incision, probably indicating a lateral accretion as observed in other studies (e.g., Abreu et al., 2003; Janocko et al., 2013; Figs. 9c and 12a). The characteristics of the Type-2 channels indicate that they are migrating laterally and have significant levee structures.

In the case of mixed channels with several different channel incisions, it is difficult to differentiate each single channel from its associated levee deposits. The concave-upward shape is mainly observed in the higher sinuosity channels. When lateral accretion was not obvious in seismic profiles, a depth slice was used to decipher their geometry (Fig. 12a). Concave-upward filled channels demonstrate lower amplitude contrast to higher amplitude surroundings, and probably indicate the presence of finer sediment infill compared to adjacent sediments (Fig. 12d).

5. Discussion

5.1 Geomorphological interpretation of the channel systems

The evolution of submarine channels usually begins by the creation of low sinuosity incisions by erosion and ends with the migration of leveed channels (Mayall et al., 2006; Deptuck et al., 2007; McHargue et al., 2011). Accordingly, submarine channels in the study area display a cyclic geomorphological evolution pattern (Table 1). The lower parts of both SU-2B-I and SU-2B-II subunits are dominated by relatively straight Type-1 channels while the

upper parts have relatively sinuous Type-2 channels. Within the relatively shallow incised Type-1 channels, no structures related to channel migration were observed. However, the relatively deeper incised Type-2 channels revealed well-developed levees, lateral migration, and accretion packages (Fig. 9). These observations suggest that Type-1 channels are an early stage channel system and Type-2 channels, mature stage. The absence of evidence for vertical stacking of U-shaped Type-2 channels above V-shaped Type-1 channels and differences in the number of identified channels for each type indicates that the channels are not markers of a channel system evolutionary history. However, they might suggest temporal variation in depositional conditions.

Clark et al. (1992) showed that fan gradient, sediment loading type and flow type play an important role in submarine channel development and that gradient is the most important factor in submarine channel development. When fan gradient decreases, sinuosity reaches its maximum and subsequently decreases. The studied unit is highly deformed due to salt-related deformation, making it difficult to constrain the paleo-seafloor gradient. However, depth slices indicate that channels predate the deformations and signify a possible low gradient paleo-seafloor (Figs. 6 and 11). Furthermore, the work of Cartwright and Jackson (2008) support this assertion. These authors restored the paleo-structures of the study area and proposed a similar bathymetry to present day seafloor with water depths of at least 500 m, implying a deep-water setting. Nonetheless, the cyclic occurrence of low and high sinuosity channels (Fig. 7) in the studied interval cannot be explained by changes in seafloor gradient. Alternatively, latitudinal control on channel evolution might be considered, as latitudinal control is strong when gradient is low (e.g., Peakall et al., 2012). However, channel peak sinuosity in the studied channels is still smaller than expected for the region, restricting latitudinal control compared to the channels studied by Peakall et al. (2012) in the Amazon, the Indus, and the Zaire fan. Therefore, the differences in flow type and sediment loading system are the main factors modulating the geomorphological characteristics of the interpreted channel system.

Furthermore, the Type-1 submarine channels are considered single channels with respective bed load systems (i.e., large sediment load, low stability, and coarse-grained sediments; following Miall, 2006). This hypothesis is corroborated by the lack of well-developed levees and more importantly, the convex-upward filling patterns at the top, which is attributed to differential compaction of the axial sandy fill and adjacent muddier deposits, presumably indicating that the channels are more sand-rich than the surrounding sediments (e.g. Posamentier, 2003; Janocko et al., 2013; Fig. 10b). On the RMS map, Type I channels show higher amplitudes that contrast to the surrounding low amplitude strata, indicating coarser

channel fill (Fig. 10b). The coarse sediment fill is also indicated by the coarsening upward stacking patterns (Fig. 4b). Hence, Type-1 channels are believed to have been formed by rapid incision with high-density turbidity currents that behave aggressively with the substratum and form erosive V-shaped incisions. This prevented lateral migration to shorten the pathway of channels and thereby decrease their sinuosity.

Miall (2006) showed that a high sinuosity meandering channel signifies a mixed load system with weak hydrodynamic conditions and that are usually infilled by fine-grained sediments. Fine-grained fans such as the Amazon and the Bengal fan, also exhibit lower sinuosity channels (Reading and Richards 1994; Piper and Normark, 2001). Type-2 channels with relatively higher sinuosity index appear as concave-upward shape filling patterns and further interpreted as evidence for fine-grained infilling, due to differential compaction of more mud-prone axial sediments than the adjacent hemipelagic deposits (*sensu* Posamentier, 2003; Janocko et al., 2013; Fig. 12c and d). The U-shaped incisions may be explained by slow and weak turbidity currents that are not as erosive as those forming the V-shaped channels and incise the sub-channel surfaces in a laterally homogeneous fashion, to form the almost flat bottoms. Such U-shaped channels are common in distal plains characterised by low dynamic conditions in the NW Mediterranean (Alonso et al., 1995). In addition, the levee structures in sinuous channels with shingled reflections and lateral migration patterns that are inferred as lateral accretion packages suggest lower flow velocity and mixed load relative to straight channels (Fig. 12b; Schumm, 1981).

5.2 Submarine channel formation and evolution mechanism

The evolution of submarine channels and related features associated with the progradation of fans or deltas towards the basin in deep-water environments is usually controlled by several intrabasinal and extrabasinal factors. These include tectonics, climate, sediment supply, sea level fluctuation and seafloor topography (e.g. Reading and Richards, 1994; Popescu et al., 2001; Heiniö and Davies, 2007; Wynn et al., 2007). Typical deep-water channels are related to long-lived feeding by rivers en-route to deep-water fans, such as the Amazon, Mississippi and Congo (Deptuck et al., 2007; Wynn et al., 2007). Relative to the study area, the modern Nile Delta started to form from the beginning of the Pliocene, and became an important sediment source to the Levant Basin (Macgregor, 2012; Fielding et al., 2018 and references therein). The submarine channels identified in this paper are located to the northeast, on the basinward extension of the Nile delta and were formed during the Pliocene (Fig. 1a). However, the lack of biostratigraphic data for the study interval, has limited

understanding of the allogenic and autogenic processes controlling the submarine channel style and overall stratigraphic organization.

The chronology of the studied interval is well constrained based on the framework presented by previous studies (e.g. Cartwright and Jackson 2008; Eruteya et al., 2015; Schattner et al., 2017; Lang et al., 2018). The northeastward decrease in sediment thickness and positioning of the submarine channels indicate that the main source of sediments is to the southwest from the Nile delta. This is consistent with the Mart and Ben Gai (1982), who showed that the Pliocene-Pleistocene sequence in the Levant Basin is predominantly detrital and its major single source for sedimentation has been the Nile River. During the early Pliocene, a deep-water turbidity basin-floor fan (the Yafo Sand Member) was deposited in the Levant area. However, this member is restricted to the southeastern part of the basin, and does not reach the study area (Frey Martinez et al., 2005; Gardosh and Druckman, 2006; Fuhrmann, 2010). Pliocene submarine channels identified in the slopes near the Nile delta are interpreted to have resulted from relative sea-level fall (Aal et al., 2000; Samuel et al., 2003; Cross et al., 2009). This is particularly valid considering that the submarine channels are only identified in SU-2B within the Pliocene succession and coeval to those observed near the Nile delta area.

5.2.1 Tectonic background and slope topography

The importance of tectonics and slope topography in controlling the formation and evolution of morphological features such as submarine channels has long been appreciated. Previous studies have shown that the Pliocene evolution of the Levant Basin is part of the post-rifting stage (Garfunkel and Derin, 1984; Garfunkel, 1998). During the Pliocene the subsidence rate in the basin peaked and the basin tilted northward by 0.6° . However, the Pliocene is still considered as being tectonically quiescent in the region with no significant tectonic events that could necessitate such channel incisions (Tibor et al., 1992; Ben-Gai et al., 2005; Tibor and Ben-Avraham 2005; Reis et al., 2013). Furthermore, a series of Pliocene channels were identified in the western Nile Cone, and interpreted as partly resulting from gravity flows related to major sea-level lowstands on a very gently inclined (1:25) slope (Aal et al., 2000; Samuel et al., 2003; Cross et al., 2009). A similar condition may have prevailed for the eastern Nile cone and the gentle slope in the margin did not play a major role in the initiation of the studied channels.

Plio-Pleistocene sequences of the Levant Basin experienced post-Messinian thin-skinned deformations and gravitational collapses of the Levant margin (Loncke et al., 2006; Frey Martinez et al., 2005; Cartwright and Jackson 2008), which probably influenced the cyclic

nature of the channels as well as their spatial distribution. The identified submarine channels are also displaced by faults without any significant shift in the depocenter and changes in the channel direction. Thus, indicating that the channels predated salt-related tectonics in the basin. This interpretation contradicts the results of Clarks (2009) and Zucker et al. (2017), who proposed that some submarine channels on the seafloor were influenced by the sub-channel deformations in the Levant Basin.

5.2.2 *Climate and sedimentation rate*

Rapid sediment supply and high sedimentation rate may increase the sediment load on a slope, leading to significant instability and large-scale sediment failure as well as turbidity channels (Reading and Richards, 1994; Miall, 2002). The Nile River crosses through equatorial Africa, tropical and arid areas that discharge sediments into the Eastern Mediterranean. However, Nile River discharge comes from the Ethiopian Highlands through the Blue Nile system (Said 1981; Williams et al., 2000; Fig. 1a). The final uplift of the Ethiopian and Somalian plateaus during the Pliocene provided important sediment source and supply to the Levant Basin through the Nile River and sediment discharge of Nile River peaked during the mid-Pliocene (Macgregor, 2011; Macgregor, 2012; Palacios, 2013; Fig 13). Additionally, the increased African Monsoon rainfall during the Pliocene was due to changes in insolation at low latitudes combined with the blocked moisture brought from the Indian Ocean (Rossignol-Strick, 1983; and references therein). The moisture was brought by the southeast trade winds due to rapid uplift of the Ethiopian plateau. This increased precipitation established suitable erosion and efficient sediment transport mechanisms for the transport of materials to the Nile delta (Partridge, 1997; Griffin, 1999; Sepulchre et al., 2006; Corti, 2009). Hence, the influence of climate on sedimentation rate and erosion has been documented for the Ethiopian Highlands and by proxy for the Nilotic sediments deposited in the study area.

5.2.3 *Sea level fluctuations*

Relative falls in sea level may result in both shoreline and basin depocenter shifts, and exposure of the shelf to erosion, forming canyons and turbidity currents, which accelerate sediment transport to the deep-water environment (Posamentier, 2001; Posamentier and Kolla, 2003; Antobreh and Krastel, 2006; Catuneanu, 2006). Nevertheless, increased sediment supply, growing fan sizes, and accelerated turbidity activity are also known to have prevailed during highstands in the Congo and Bengal fans (Van Weering and Van Iperen, 1984; Weber et al., 1997). The gentle slope morphology and lack of evidence for significant mid-Pliocene failures

has excluded the possibility of submarine canyon and channel development during the highstand (Samuel et al., 2003). In the case of the Nile delta slope, several submarine channels have mainly attributed to relative sea level fall (e.g., Aal et al., 2000; Samuel et al., 2003). An apparent sea level drop and records of deep-sea oxygen isotopes during the mid-Pliocene has also been documented (Miller et al., 2011; Fig 13). Therefore, relative sea level fluctuations also played an important role in the occurrence and extension of submarine channels in the study area.

Considering the sediment discharge rate and thickness of the studied Pliocene unit, we infer that the two observed cycles characterised by channels and their respective geomorphological evolution, may have taken at least one million year (Fig. 12). Relative sea-level fluctuations (especially on an orbital scale; Tuenter et al., 2003) likely influenced the channel development. Also, relatively fast uplift of the Ethiopian plateau might have contributed to the sedimentation rate, as well to the initiation of a network of the submarine channels. However, none of these tectonic or climatic processes could produce the cyclic distribution and variability of the deep-sea turbidity system responses identified in this study within a timeframe of half million years. Orbitally forced sea level fluctuations can cause cyclic change within hundreds of thousands years (fourth order cycles) and plays an important role in the systematic and cyclic development of deep-water sequences (Vail et al., 1977; Posamentier et al., 2000; Catuneanu, 2006; Posamentier and Kolla 2003; Miall, 2013). Badalini et al. (2000) showed that frequent alternation of aggradation and erosion are possibly related to flow parameters on a thousand-year timescale.

Accordingly, the evolution of the different channel types can be explained by sea level fluctuations. During regressions, turbidity currents in the deep basin are dominated by higher density flows due to increased sediment supply (sediment load > energy of the flow), lower hydraulic pressures and abundance in coarser grain size sediments (Catuneanu, 2006; Wang et al., 2016). Submarine channels during lowstands are highly erosive, display lower sinuosity patterns, and comprise a higher sand/mud ratio (e.g., Shanley and McCabe, 1994; Tripsanas et al., 2006), which are represented by the V-shaped Type-1 channels (Fig. 13). In contrast, during periods of relative sea level rise, the shoreline and depocenter shift landward with significantly less and finer sediments delivered to the deep-water environment through turbidity currents. These turbidity currents tend to be low-density and under-loaded on the steep continental slope (flow energy > sediment load, which causes erosion), but become overloaded on the basin floor (sediment load > flow energy). The low-density turbidity flows travel farther into the basin relative to the high-density flows that formed during the regression, because the higher

proportion of mud sustains the construction of levees over larger distances (Catuneanu, 2006; Fig. 13). These turbidity channels, therefore, tend to be overloaded/aggradational on the low-gradient basin floor (sediment load < flow energy). Hence, submarine channels in this period displayed a lateral meandering morphology, a lower sinuosity, and were mostly infilled with finer sediments compared to the surroundings (Shanley and McCabe, 1994; Catuneanu, 2006), similar to the Type-2 channels. When sea level reached its relative high, turbidity currents became very weak and did not travel as far as the transgressive low-density currents, leaving the distal basin for hemipelagic deposition, represented by the uninterrupted uniform horizon B (Fig. 4). During the relative sea level fall, this cycle repeats again until the channels cease to be active under the influence of sea level fluctuations, sedimentation rate and climatic change.

5.3. Evolutionary model for the interpreted channel-belt interval

Following the end of the Messinian salinity crisis, sediment discharge from the Nile to the Mediterranean Sea increased, but submarine channels remained at low activity, mainly due to rising sea level, with hemipelagic sediments (unit SU-2A) dominating the entire deep sea environment during this period (Fig. 14a). Sediment discharge peaked during the mid-Pliocene, probably as a result of the last uplift stage of the Ethiopian plateau (Macgregor, 2012; Palacios, 2013) and increased east African monsoon activity (Tuenter et al., 2003). Meanwhile, relative sea level fell, delivering coarser sediments to the deep basin and increasing the possibility of turbidity channel development (Fig. 14b to f). The turbidity currents initially had higher velocities and formed relatively straight, erosive V-shaped channels, which were mostly infilled with coarser sediments (Fig. 14b). Subsequently, orbital-forced sea levels started to rise (higher order cycle), which led to the decrease in turbidity current velocity and the formation of sinuous U-shaped depositional channels infilled with finer sediments (Fig. 14c). In the final stage, the deep-sea environment was characterised by the deposition of about 20 m of hemipelagic sediments (Fig. 14d). This cycle repeated, with the alternate deposition of Type-1 and Type-2 channels (Fig. 14e and f), until climate forced an increase in sediment discharge from the Nile and sea level rose to its maximum during this period (Fig. 14g).

6. Conclusions

Integrated analysis of a high-resolution, 3-D seismic reflection dataset and borehole data from the Levant Basin offshore central Israel has revealed a duplex submarine channel belt within the Pliocene succession. The channels were likely developed in response to lowering sea level and increased sediment discharge as result of increased humidity and

precipitation in the upper-Nile river watershed. Geomorphologic characterization of the channels includes two recognised types: V-shaped Type-1 and U-shaped Type-2 channels, with respective low sinuosity-isolated channels and higher sinuosity-depositional channels. Type-1 channels dominate the lower part of each unit, while Type-2 channels are prevalent at the upper parts, hence indicating a periodic sea level change during the Pliocene. The channels in the lower parts of each subunit are inferred to have been generated during periods of orbitally forced sea level fall, while the channels in the upper part were carved during relative sea level rise. The long-term occurrence of channels in the studied area is likely controlled by relative sea level fluctuations, coupled by increased Nile River sediment supply. The possible influence of a rapid uplift stage of the Ethiopian plateau is taken into consideration, as well as increase in the east African monsoon activity during the Pliocene. The high-resolution investigation of turbidity channels in deep marine environments, such as this study for the Pliocene in the Levant Basin, serves as an important tool for better understanding of the different mechanisms behind source-to-sink processes in basins worldwide. Moreover, the current work provides a novel technique to measure the impact and magnitude of orbital-scale climate variability on deep marine sediments.

Acknowledgement

The authors are grateful to ILDC, Modi'in Energy and GGR for graciously granting us the permission to show the geophysical dataset. The authors are grateful to M. Reshef and Y. Makovsky with help with the dataset and O. Bialik for fruitful discussions. We also thank Schlumberger, Paradigm and IHS Kingdom for granting academic licenses of their respective seismic processing and interpretation software packages to the Department of Marine Geosciences, University of Haifa. KOO hereby expresses his sincere appreciation to the European Cooperation in Science and Technology (COST) under the framework of COST Action CA15103 (MEDSALT) for partially supporting his visit to the University of Haifa. This project form part of a Marie Curie Career Integration Grants (CIG) Call: FP7-PEOPLE-2011-CIG for NW, which supported the MSc thesis of YN and the PhD thesis of OEE. We are deeply grateful to the Editor, Prof Michele Rebesco and two anonymous reviewers for their suggestions and reviews that greatly improved the outlook of the manuscript.

ACCEPTED MANUSCRIPT

References

- Aal, A.A., Barkooky, A.E., Gerrits, M., Meyer, H., Schwander, M., Zaki, H., 2000. Tectonic evolution of the Eastern Mediterranean Basin and its significance for hydrocarbon prospectivity in the ultradeepwater of the Nile Delta. *Lead. Edge* 19, 1086–1102.
- Abreu, V., Sullivan, M., Pirmez, C., Mohrig, D., 2003. Lateral accretion packages (LAPs): an important reservoir element in deep water sinuous channels. *Mar. Pet. Geol.* 20, 631–648.
- Alonso, B., Canals, M., Palanques, A., Rehault, J.-P., 1995. A Deep-sea Channel in the Northwestern Mediterranean Sea: Morphology and seismic structure of the Valencia Channel and its surroundings. *Mar. Geophys. Res.* 17, 469–484.
- Antobreh, A.A., Krastel, S., 2006. Morphology, seismic characteristics and development of Cap Timiris Canyon, offshore Mauritania: A newly discovered canyon preserved-off a major arid climatic region. *Mar. Pet. Geol.* 23, 37–59.
- Adeogba, A.A., McHargue, T.R., Graham, S.A., 2005. Transient fan architecture and depositional controls from near-surface 3-D seismic data, Niger Delta continental slope. *AAPG Bull.* 89, 627–643.
- Babonneau, N., Savoye, B., Cremer, M., Bez, M., 2010. Sedimentary Architecture in Meanders of a Submarine Channel: Detailed Study of the Present Congo Turbidite Channel (Zaiango Project). *J. Sediment. Res.* 80, 852–866.
- Babonneau, N., Savoye, B., Cremer, M., Klein, B., 2002. Morphology and architecture of the present canyon and channel system of the Zaire deep-sea fan. *Mar. Pet. Geol.* 19, 445–467.
- Bain, H.A., Hubbard, S.M., 2016. Stratigraphic evolution of a long-lived submarine channel system in the Late Cretaceous Nanaimo Group, British Columbia, Canada. *Sediment. Geol.* 337, 113–132.
- Ben-Gai, Y., Ben-Avraham, Z., Buchbinder, B., Kendall, C.G.S.C., 2005. Post-Messinian evolution of the Southeastern Levant Basin based on two-dimensional stratigraphic simulation. *Mar. Geol.* 221, 359–379.
- Bertoni, C., Cartwright, J.A., 2005. 3D seismic analysis of circular evaporite dissolution structures, Eastern Mediterranean. *J. Geol. Soc. London* 162, 909–926.
- Blum, M.D., Törnqvist, T.E., 2000. Fluvial responses to climate and sea-level change: a review and look forward. *Sedimentology* 47, 2–48.
- Bouma, A.H., 2001. Fine-grained submarine fans as possible recorders of long- and short-term climatic changes. *Glob. Planet. Change* 28, 85–91.

- Brenchley, P.J., Marshall, J.D., Harper, D., 2006. A late Ordovician (Hirnantian) karstic surface in a submarine channel, recording glacio - eustatic sea - level changes: Meifod, central Wales. *Geological*.
- Brown, A.R., 2004. Interpretation of Three-dimensional Seismic Data. American Association of Petroleum Geologists and the Society of Exploration Geophysicists.
- Carter, D.C., 2003. 3-D seismic geomorphology: Insights into fluvial reservoir deposition and performance, Widuri field, Java Sea. *AAPG Bull.* 87, 909–934.
- Cartwright, J.A., Jackson, M.P.A., 2008. Initiation of gravitational collapse of an evaporite basin margin: The Messinian saline giant, Levant Basin, eastern Mediterranean. *Geol. Soc. Am. Bull.* 120, 399–413.
- Catuneanu, O., 2006. Principles of Sequence Stratigraphy. Elsevier.
- Clark, I.R., Cartwright, J.A., 2009. Interactions between submarine channel systems and deformation in deepwater fold belts: Examples from the Levant Basin, Eastern Mediterranean Sea. *Mar. Pet. Geol.* 26, 1465–1482.
- Clark, J.D., Kenyon, N.H., Pickering, K.T., 1992. Quantitative analysis of the geometry of submarine channels: Implications for the classification of submarine fans. *Geology* 20, 633–636.
- Corti, G., 2009. Continental rift evolution: From rift initiation to incipient break-up in the Main Ethiopian Rift, East Africa. *Earth-Sci. Rev.* 96, 1–53.
- Covault, J.A., 2011. Submarine fans and canyon-channel systems: a review of processes, products, and models. *Nature Education Knowledge* 3, 4.
- Covault, J.A., Kostic, S., Paull, C.K., Ryan, H.F., Fildani, A., 2014. Submarine channel initiation, filling and maintenance from sea-floor geomorphology and morphodynamic modelling of cyclic steps. *Sedimentology* 61, 1031–1054.
- Cross, N.E., Cunningham, A., Cook, R.J., Taha, A., 2009. Three-dimensional seismic geomorphology of a deep-water slope-channel system: The Sequoia field, offshore west Nile Delta, Egypt. *AAPG*.
- Damuth, J.E., Kolla, V., Flood, R.D., Kowsmann, R.O., 1983. Distributary channel meandering and bifurcation patterns on the Amazon deep-sea fan as revealed by long-range side-scan sonar (GLORIA).
- Darmadi, Y., Willis, B.J., Dorobek, S.L., 2007. Three-Dimensional Seismic Architecture of Fluvial Sequences on the Low-Gradient Sunda Shelf, Offshore Indonesia. *J. Sediment. Res.* 77, 225–238.

- deMenocal, P.B., 1995. Plio-Pleistocene African Climate. *Science* 270, 53–59.
- Dutton, A., Lambeck, K., 2012. Ice volume and sea level during the last interglacial. *Science* 337, 216–219.
- Deptuck, M.E., Steffens, G.S., Barton, M., Pirmez, C., 2003. Architecture and evolution of upper fan channel-belts on the Niger Delta slope and in the Arabian Sea. *Mar. Pet. Geol.* 20, 649–676.
- Deptuck, M.E., Sylvester, Z., Pirmez, C., O’Byrne, C., 2007. Migration–aggradation history and 3-D seismic geomorphology of submarine channels in the Pleistocene Benin-major Canyon, western Niger Delta slope. *Mar. Pet. Geol.* 24, 406–433.
- Di Celma, C., Cantalamessa, G., Didaskalou, P., Lori, P., 2010. Sedimentology, architecture, and sequence stratigraphy of coarse-grained, submarine canyon fills from the Pleistocene (Gelasian-Calabrian) of the Peri-Adriatic basin, central Italy. *Mar. Pet. Geol.* 27, 1340–1365.
- Druckman, Y., Buchbinder, B., Martinotti, G.M., Tov, R.S., Aharon, P., 1995. The buried Afiq Canyon (eastern Mediterranean, Israel): a case study of a Tertiary submarine canyon exposed in Late Messinian times. *Mar. Geol.* 123, 167–185.
- Ducassou, E., Migeon, S., Capotondi, L., Mascle, J., 2013. Run-out distance and erosion of debris-flows in the Nile deep-sea fan system: Evidence from lithofacies and micropalaeontological analyses. *Mar. Pet. Geol.* 39, 102–123.
- Ducassou, E., Migeon, S., Mulder, T., Murat, A., Capotondi, L., Bernasconi, S.M., Mascle, J., 2009. Evolution of the Nile deep-sea turbidite system during the Late Quaternary: influence of climate change on fan sedimentation. *Sedimentology* 56, 2061–2090.
- Eruteya, O.E., Safadi, M., Waldmann, N., Makovsky, Y., Ben-Avraham, Z., 2016. Seismic Geomorphology of the Israel Slump Complex in the Levant Basin (SE Mediterranean), in: Lamarche, G., Mountjoy, J., Bull, S., Hubble, T., Krastel, S., Lane, E., Micallef, A., Moscardelli, L., Mueller, C., Pecher, I., Woelz, S. (Eds.), *Submarine Mass Movements and Their Consequences, Advances in Natural and Technological Hazards Research*. Springer International Publishing, pp. 39–47.
- Eruteya, O.E., Waldmann, N., Schalev, D., Makovsky, Y., Ben-Avraham, Z., 2015. Intra- to post-Messinian deep-water gas piping in the Levant Basin, SE Mediterranean. *Mar. Pet. Geol.* 66, Part 1, 246–261.
- Feng, Y.E., Yankelzon, A., Steinberg, J., Reshef, M., 2016. Lithology and characteristics of the Messinian evaporite sequence of the deep Levant Basin, eastern Mediterranean. *Mar. Geol.* 376, 118–131.

- Feng, Z.-Q., 2000. An investigation of fluvial geomorphology in the Quaternary of the Gulf of Thailand, with implications for river classification. University of Reading.
- Fielding, L., Najman, Y., Millar, I., Butterworth, P., Garzanti, E., Vezzoli, G., Barfod, D., Kneller, B., 2018. The initiation and evolution of the River Nile. *Earth Planet. Sci. Lett.* 489, 166–178.
- Flood, R.D., Damuth, J.E., 1987. Quantitative characteristics of sinuous distributary channels on the Amazon deep-sea fan. Geological Society of America.
- Folkman, Y., Mart, Y., 2008. Newly recognized eastern extension of the Nile deep-sea fan. *Geology* 36, 939–942.
- Frey Martinez, J., Cartwright, J., Hall, B., 2005. 3D seismic interpretation of slump complexes: examples from the continental margin of Israel. *Basin Res.* 17, 83–108.
- Fuhrmann, A.R., 2010. The Origin of the Lower Pliocene Deepwater Andromeda Mound Complex, Levant Basin, Eastern Mediterranean Sea, Offshore Israel. University of Colorado at Boulder, Ann Arbor, United States.
- Gamboa, D., Alves, T.M., 2015. Spatial and dimensional relationships of submarine slope architectural elements: A seismic-scale analysis from the Espírito Santo Basin (SE Brazil). *Mar. Pet. Geol.* 64, 43–57.
- Gamboa, D., Alves, T.M., Cartwright, J., 2012. A submarine channel confluence classification for topographically confined slopes. *Mar. Pet. Geol.* 35, 176–189.
- Gardosh, M., Druckman, Y., Buchbinder, B., Rybakov, M., 2008a. The Levant Basin offshore Israel: stratigraphy, structure, tectonic evolution and implications for hydrocarbon exploration. Geophysical Institute of Israel.
- Gardosh, M., Druckman, Y., Buchbinder, B., Calvo, R., 2008b. The Oligo-Miocene deepwater system of the Levant Basin. *Geological Survey of Israel* 33, 1–73.
- Garfunkel, Z., 1998. Constrains on the origin and history of the Eastern Mediterranean basin. *Tectonophysics* 298, 5–35.
- Garfunkel, Z., Derin, B., 1984. Permian-early Mesozoic tectonism and continental margin formation in Israel and its implications for the history of the Eastern Mediterranean. Geological Society, London, Special Publications 17, 187–201.
- Gaullier, V., Mart, Y., Bellaiche, G., Mascle, J., Vendeville, B.C., Zitter, T., Second Leg Prismed II Scientific Party, 2000. Salt tectonics in and around the Nile deep-sea fan: insights from the PRISMED II cruise. Geological Society, London, Special Publications 174, 111–129.

- Gradmann, S., Hübscher, C., Ben-Avraham, Z., Gajewski, D., Netzeband, G., 2005. Salt tectonics off northern Israel. *Mar. Pet. Geol.* 22, 597–611.
- Griffin, D.L., 1999. The late Miocene climate of northeastern Africa: unravelling the signals in the sedimentary succession. *J. Geol. Soc. London* 156, 817–826.
- Gvirtzman, Z., Reshef, M., Buch-Leviatan, O., Ben-Avraham, Z., 2013. Intense salt deformation in the Levant Basin in the middle of the Messinian Salinity Crisis. *Earth Planet. Sci. Lett.* 379, 108–119.
- Gvirtzman, Z., Reshef, M., Buch-Leviatan, O., Groves-Gidney, G., Karcz, Z., Makovsky, Y., Ben-Avraham, Z., 2015. Bathymetry of the Levant basin: interaction of salt-tectonics and surficial mass movements. *Mar. Geol.* 360, 25–39.
- Hansen, L., Janocko, M., Kane, I., Kneller, B., 2017. Submarine channel evolution, terrace development, and preservation of intra-channel thin-bedded turbidites: Mahin and Avon channels, offshore Nigeria. *Mar. Geol.* 383, 146–167.
- Harishidayat, D., Omosanya, K.O., Johansen, S.E., 2015. 3D seismic interpretation of the depositional morphology of the Middle to Late Triassic fluvial system in Eastern Hammerfest Basin, Barents Sea. *Mar. Pet. Geol.* 68, 470–479.
- Heiniö, P., Davies, R.J., 2007. Knickpoint migration in submarine channels in response to fold growth, western Niger Delta. *Mar. Pet. Geol.* 24, 434–449.
- Hodgson, D.M., Di Celma, C.N., Brunt, R.L., Flint, S.S., 2011. Submarine slope degradation and aggradation and the stratigraphic evolution of channel–levee systems. *J. Geol. Soc. London* 168, 625–628.
- Hsu, K.J., Montadert, L., Bernoulli, D., Cita, M.B., Erikson, A., Garrison, R.E., Kidd, R.B., Melieres, F., Muller, C., Wright, R., 1978. History of the Mediterranean Salinity Crisis, in: Hsu, K., Montadert, L., et al. (Eds.), *Initial Reports of the Deep Sea Drilling Project*, 42 Pt. 1, *Initial Reports of the Deep Sea Drilling Project*. U.S. Government Printing Office.
- Hübscher, C., Spieß, V., Breitzke, M., Weber, M.E., 1997. The youngest channel-levee system of the Bengal Fan: results from digital sediment echosounder data. *Mar. Geol.* 141, 125–145.
- Janocko, M., Nemeč, W., Henriksen, S., Warchoń, M., 2013. The diversity of deep-water sinuous channel belts and slope valley-fill complexes. *Mar. Pet. Geol.* 41, 7–34.
- J.K. Hall, S. Lippman, M. Gardosh, G. Tibor, A.R. Sade, H. Sade *A New Bathymetric Map for the Israeli EEZ : Preliminary Results Ministry of National Infrastructures, Energy and Water Resources (2015)*

- Katz, O., Reuven, E., Aharonov, E., 2015. Submarine landslides and fault scarps along the eastern Mediterranean Israeli continental-slope. *Mar. Geol.* 369, 100–115.
- Kellner, A., El Khawaga, H., Brink, G., Brink-Larsen, S., Hesham, M., El Saad, H.A., Atef, A., Young, H., Finlayson, B., 2009. Depositional History of the West Nile Delta--Upper Oligocene to Upper Pliocene. *Search and Discovery Article* 30092.
- Kolla, V., Posamentier, H.W., Wood, L.J., 2007. Deep-water and fluvial sinuous channels—Characteristics, similarities and dissimilarities, and modes of formation. *Mar. Pet. Geol.* 24, 388–405.
- Lang, G., Lazar, M., Schattner, U., 2018. Structural implications of strain localization towards a continental transform fault: The example of the shift between the Levant margin and the Dead Sea Fault plate boundary. *Mar. Pet. Geol.* 89, 402–414.
- Larrasoana, J.C., Parés, J.M., Millán, H., Del Valle, J., Pueyo, E.L., 2003. Paleomagnetic, structural, and stratigraphic constraints on transverse fault kinematics during basin inversion: The Pamplona Fault (Pyrenees, north Spain). *Tectonics* 22.
- Li, S., Gong, C., 2016. Flow dynamics and sedimentation of lateral accretion packages in sinuous deep-water channels: A 3D seismic case study from the northwestern South China Sea margin. *J. Asian Earth Sci.* 124, 233–246.
- Lofi, J., Déverchère, J., Gaullier, V., Gillet, H., Gorini, C., Guennoc, P., Loncke, L., Maillard, A., Sage, F., Thinon, I., 2011. Seismic atlas of the Messinian Salinity Crisis markers in the Mediterranean and Black Seas. *Société Géologique de France*.
- Loncke, L., Gaullier, V., Bellaiche, G., Mascle, J., 2002. Recent depositional patterns of the Nile deep-sea fan from echo-character mapping. *AAPG Bull.* 86.
- Loncke, L., Gaullier, V., Mascle, J., Vendeville, B., Camera, L., 2006. The Nile deep-sea fan: An example of interacting sedimentation, salt tectonics, and inherited subsalt paleotopographic features. *Mar. Pet. Geol.* 23, 297–315.
- Macgregor, D., 2011. Rift shoulder source to prodelta sink: The Cenozoic development of the Nile drainage system. *Search and Discovery Article* 50506.
- Macgregor, D.S., 2012. The development of the Nile drainage system: integration of onshore and offshore evidence. *Pet. Geosci.* 18, 417–431.
- Mayall, M., Jones, E., Casey, M., 2006. Turbidite channel reservoirs—Key elements in facies prediction and effective development. *Mar. Pet. Geol.* 23, 821–841.
- Mayall, M., Lonergan, L., Bowman, A., James, S., Mills, K., Primmer, T., Pope, D., Rogers, L., Skeene, R., 2010. The response of turbidite slope channels to growth-induced seabed topography. *Bull. Am. Assoc. Hist. Nurs.* 94, 1011–1030.

- McHargue, T., Pyrcz, M.J., Sullivan, M.D., Clark, J.D., Fildani, A., Romans, B.W., Covault, J.A., Levy, M., Posamentier, H.W., Drinkwater, N.J., 2011. Architecture of turbidite channel systems on the continental slope: Patterns and predictions. *Mar. Pet. Geol.* 28, 728–743.
- Miall, A.D., 2013. *Principles of Sedimentary Basin Analysis*. Springer Science & Business Media.
- Miall, A.D., 2016. Stratigraphy: The Modern Synthesis, in: *Stratigraphy: A Modern Synthesis*. Springer International Publishing, pp. 311–370.
- Miall, A.D., 2002. Architecture and sequence stratigraphy of Pleistocene fluvial systems in the Malay Basin, based on seismic time-slice analysis. *AAPG Bull.* 86.
- Mitchum, R.M., Jr, Vail, P.R., Sangree, J.B., 1977. Seismic stratigraphy and global changes of sea level: Part 6. Stratigraphic interpretation of seismic reflection patterns in depositional sequences: Section 2. Application of seismic reflection configuration to stratigraphic interpretation.
- Miller, K.G., Mountain, G.S., Wright, J.D., Browning, J.V., 2011. A 180-Million-Year Record of Sea Level and Ice Volume Variations from Continental Margin and Deep-Sea Isotopic Records. *Oceanography* 24, 40–53.
- Mueller, J.E., 1968. An introduction to the hydraulic and topographic sinuosity indexes. *Ann. Assoc. Am. Geogr.* 58, 371–385.
- Mulder, T and J Alexander; 2001, “The physical character of subaqueous sedimentary density flows and their deposits”; *Sedimentology*: 48, 269-299
- NASA LP DAAC. Global data explorer (Powered by GeoBrain) Retrieved 2013, November 12, from <http://gdex.cr.usgs.gov/gdex/>.
- Omosanya, K.O., Alves, T.M., 2013. A 3-dimensional seismic method to assess the provenance of Mass-Transport Deposits (MTDs) on salt-rich continental slopes (Espírito Santo Basin, SE Brazil), *Marine and Petroleum Geology* 44, 223- 239 <http://dx.doi.org/10.1016/j.marpetgeo.2013.02.006>
- Palacios, Z.H., 2013. *Climate change as a controlling parameter in sediment supply: the Nile Province*. University of Aberdeen.
- Partridge, T.C., 1997. Late Neogene Uplift in Eastern and Southern Africa and Its Paleoclimatic Implications, in: *Tectonic Uplift and Climate Change*. Springer, Boston, MA, pp. 63–86
- Peakall, J., Sumner, E.J., 2015. Submarine channel flow processes and deposits: A process-product perspective. *Geomorphology* 244, 95–120.

- Pickering, K., Coleman, J., Cremer, M., Droz, L., Kohl, B., Normark, W., O'Connell, S., Stow, D., Meyer-Wright, A., 1986. A high sinuosity, laterally migrating submarine fan channel-levee-overbank: results from DSDP Leg 96 on the Mississippi Fan, Gulf of Mexico. *Mar. Pet. Geol.* 3, 3–18.
- Piper, D.J.W., Normark, W.R., 2001. Sandy fans--from Amazon to Hueneme and beyond. *AAPG Bull.* 85, 1407–1438.
- Popescu, I., Lericolais, G., Panin, N., Wong, H.K., Droz, L., 2001. Late Quaternary channel avulsions on the Danube deep-sea fan, Black Sea. *Mar. Geol.* 179, 25–37.
- Posamentier, H.W., 2003. Depositional elements associated with a basin floor channel-levee system: case study from the Gulf of Mexico. *Mar. Pet. Geol.* 20, 677–690.
- Posamentier, H.W., 2001. Lowstand alluvial bypass systems: incised vs. unincised. *AAPG Bull.* 85, 1771–1793.
- Posamentier, H.W., Davies, R.J., Cartwright, J.A., Wood, L., 2007. Seismic geomorphology - an overview. Geological Society, London, Special Publications 277, 1–14.
- Posamentier, H.W., Kolla, V., 2003. Seismic Geomorphology and Stratigraphy of Depositional Elements in Deep-Water Settings. *J. Sediment. Res.* 73, 367–388.
- Posamentier, H.W., Wisman, P.S., Plawman, T., 2000. Deep Water Depositional Systems2Ultra Deep Makassar Strait, Indonesia.
- Pratson, L.F., Coakley, B.J., 1996. A model for the headward erosion of submarine canyons induced by downslope-eroding sediment flows. *Geol. Soc. Am. Bull.* 108, 225–234.
- Qin, Y., Alves, T.M., Constantine, J., Gamboa, D., 2016. Quantitative seismic geomorphology of a submarine channel system in SE Brazil (Espírito Santo Basin): Scale comparison with other submarine channel systems. *Mar. Pet. Geol.* 78, 455–473.
- Reading, H.G., Richards, M., 1994. Turbidite systems in deep-water basin margins classified by grain size and feeder system. *AAPG Bull.* 78, 792–822.
- Reiche, S., Hübscher, C., Beitz, M., 2014. Fault-controlled evaporite deformation in the Levant Basin, Eastern Mediterranean. *Mar. Geol.* 354, 53–68.
- Richards, M., Bowman, M., 1998. Submarine fans and related depositional systems ii: variability in reservoir architecture and wireline log character. *Mar. Pet. Geol.* 15, 821–839
- Rossignol-Strick, M., 1983. African monsoons, an immediate climate response to orbital insolation. *Nature* 304, 46.
- Roveri, M., Flecker, R., Krijgsman, W., Lofi, J., Lugli, S., Manzi, V., Sierro, F.J., Bertini, A., Camerlenghi, A., De Lange, G., Govers, R., Hilgen, F.J., Hübscher, C., Meijer, P.T.,

- Stoica, M., 2014. The Messinian Salinity Crisis: Past and future of a great challenge for marine sciences. *Mar. Geol.* 352, 25–58.
- Said, R., 1981. Introduction, in: *The GEOLOGICAL EVOLUTION of the RIVER NILE*. Springer New York, pp. 1–11.
- Saller, A.H., Noah, J.T., Ruzuar, A.P., Schneider, R., 2004. Linked lowstand delta to basin-floor fan deposition, offshore Indonesia: An analog for deep-water reservoir systems. *AAPG Bull.* 88, 21–46.
- Samorn, A., 2006. Fluvial reservoir architecture from near-surface 3-D seismic data. Block B8/32, Gulf of Thailand: MS thesis, Colorado School of Mines, Golden.
- Schattner, U., Lang, G., Lazar, M., 2017. Pliocene or Pleistocene, That Is the Question – New Constraints from the Eastern Mediterranean, in: Yehouda Enzel, O.B.Y. (Ed.), *Quaternary of the Levant: Environments, Climate Change, and Humans*. Cambridge University Press, pp. 63–74
- Schumm, S.A., 1993. River Response to Baselevel Change: Implications for Sequence Stratigraphy. *J. Geol.* 101, 279–294.
- Schumm, S.A., 1981. Evolution and response of the fluvial system, sedimentologic implications.
- Schumm, S.A., Harvey, M.D., Watson, C.C., 1984. Incised channels: morphology, dynamics, and control.
- Schwenk, T., Spieß, V., Hübscher, C., Breitzke, M., 2003. Frequent channel avulsions within the active channel–levee system of the middle Bengal Fan—an exceptional channel–levee development derived from Parasound and Hydrosweep data. *Deep Sea Res. Part 2 Top. Stud. Oceanogr.* 50, 1023–1045.
- Sepulchre, P., Ramstein, G., Fluteau, F., Schuster, M., Tiercelin, J.-J., Brunet, M., 2006. Tectonic uplift and Eastern Africa aridification. *Science* 313, 1419–1423.
- Shanley, K.W., McCabe, P.J., 1994. Perspectives on the sequence stratigraphy of continental strata. *AAPG Bull.* 78, 544–568.
- Shepard, F.P., Emery, K.O., 1973. Congo submarine canyon and fan valley. *AAPG Bull.* 57, 1679–1691.
- Sylvester, Z., Covault, J.A., 2016. Development of cutoff-related knickpoints during early evolution of submarine channels. *Geology* 44, 835–838.
- Sylvester, Z., Pirmez, C., Cantelli, A., 2011. A model of submarine channel-levee evolution based on channel trajectories: Implications for stratigraphic architecture. *Mar. Pet. Geol.* 28, 716–727.

- Taner, M.T., 2001. Seismic attributes. *CSEG recorder* 26, 48–56.
- Tibor, G., Ben-Avraham, Z., 2005. Late Tertiary paleodepth reconstruction of the Levant margin off Israel. *Mar. Geol.* 221, 331–347.
- Tibor, G., Ben-Avraham, Z., Steckler, M., Fligelman, H., 1992. Late Tertiary subsidence history of the Southern Levant Margin, Eastern Mediterranean Sea, and its implications to the understanding of the Messinian event. *J. Geophys. Res.* 97, 17593–17614.
- Tripsanas, Efthymios K. and David J.W. Piper 2006, "formation of Cohesionless Debris Flows and Turbidity Currents from Sediment Failures: A Case Study from the Continental Margin of Southwest Orphan basin, Labrador Sea", *SEPM Research Symposium: The Significance of Mass Transport Deposits in Deepwater Environments II*, AAPG Annual Convention, April 9-12, 2006 Technical Program
- Tuenter, E., Weber, S.L., Hilgen, F.J., Lourens, L.J., 2003. The response of the African summer monsoon to remote and local forcing due to precession and obliquity. *Glob. Planet. Change* 36, 219–235.
- Vail, P.R., Mitchum, R.M., Jr, Thompson, S., III, 1977. *Seismic Stratigraphy and Global Changes of Sea Level: Part 4. Global Cycles of Relative Changes of Sea Level.: Section 2. Application of Seismic Reflection Configuration to Stratigraphic Interpretation.*
- Van Strien, W.J., 2010. The impact of discharge, supply and base-level cyclicity on (fan) delta development. dspace.library.uu.nl.
- Van Weering, T., Van Iperen, J., 1984. *Fine-grained sediments of the Zaire deep-sea fan, southern Atlantic Ocean.* Geological Society, London.
- Wang, L., Wang, Z., Yu, S., Ngia, N.R., 2016. Seismic responses and controlling factors of Miocene deepwater gravity-flow deposits in Block A, Lower Congo Basin. *J. Afr. Earth. Sci.* 120, 31–43.
- Weaver, P.P.E., Wynn, R.B., Kenyon, N.H., Evans, J., 2000. Continental margin sedimentation, with special reference to the north-east Atlantic margin. *Sedimentology* 47, 239–256.
- Weber, M.E., Wiedicke, M.H., Kudrass, H.R., Hübscher, C., Erlenkeuser, H., 1997. Active growth of the Bengal Fan during sea-level rise and highstand. *Geology* 25, 315–318.
- Weimer, P., Slatt, R.M., Bouroullec, R., 2007. *Introduction to the petroleum geology of deepwater settings.* AAPG/Datapages Tulsa.
- Williams, M.A.J., Adamson, D., Cock, B., McEvedy, R., 2000. Late Quaternary environments in the White Nile region, Sudan. *Glob. Planet. Change* 26, 305–316.

- Wood, L.J., 2007. Quantitative Seismic Geomorphology of Pliocene and Miocene Fluvial Systems in the Northern Gulf of Mexico, U.S.A. *J. Sediment. Res.* 77, 713–730.
- Wynn, R.B., Cronin, B.T., Peakall, J., 2007. Sinuous deep-water channels: Genesis, geometry and architecture. *Mar. Pet. Geol.* 24, 341–387.
- Zeng, H., 2001. From seismic stratigraphy to seismic sedimentology: a sensible transition.
- Zeng, H., Henry, S.C., Riola, J.P., 1998. Stratal slicing, Part II: Real 3-D seismic data. *Geophysics* 63, 514–522.
- Zervas, I., Omosanya, K.O., Lippard, S.J., Johansen, S.E., 2018. Fault kinematics and localised inversion within the Troms-Finnmark Fault Complex, SW Barents Sea. *J. Struct. Geol.* 109, 10–26.
- Zucker, E., Gvirtzman, Z., Steinberg, J., Enzel, Y., 2017. Diversion and morphology of submarine channels in response to regional slopes and localized salt tectonics, Levant Basin. *Mar. Pet. Geol.* 81, 98–111.
- Zühlsdorff, C., Wien, K., Stuu, J.-B.W., Henrich, R., 2007. Late Quaternary sedimentation within a submarine channel–levee system offshore Cap Timiris, Mauritania. *Mar. Geol.* 240, 217–234.
- Zviely, D., Kit, E., Klein, M., 2007. Longshore sand transport estimates along the Mediterranean coast of Israel in the Holocene. *Mar. Geol.* 238, 61–73.

Figure Captions

Figure 1. (a) 30 Arc-Second Elevation (GTOPO30) digital elevation model (DEM) of Africa (NASA LP DAAC, 2013). The blue line represents the Nile River; the black rectangular represents the location of Figure 1b. (b) Bathymetry map of the Levant Basin (modified from Hall et al., 2015). Locations of the 2-D tow lines and 3-D seismic survey area are represented by black straight lines and red rectangular, respectively. Location of the Myra-1 well is also shown. (c) Seafloor map of the study area from 3-D seismic data (location in Figure 1b), with location of seismic sections from 3-D data. Normal faults and present-day seafloor channels are shown.

Figure 2. Interpreted SE-NW (a) and NE-SW (b) 2-D seismic profiles. The Pliocene and Pleistocene boundary is based on the interpretation of Schattner et al. (2017) and Cartwright and Jackson (2008).

Figure 3. Schematic drawing showing the methods adopted to identify and measure the morphometric parameters of the submarine channel systems in this study. (a) Plan view map showing the morphometric parameters: channel sinuous length ($L1$), and channel straight length ($L2$). Sinuosity (SI) was calculated as the ratio of $L1$ to $L2$. (b) Section view map showing the method adopted to measure the channel relief (CR) and channel maximum width (CW), from the cross-section. (c) Simplified illustration of the difference between two horizontal “depth” slices and an iso-propositional slice. Depth slices are horizontal slices that are taken through the original 3-D seismic volume, whereas the iso-proportional slices are obtained by slicing between two non-parallel reflections. Notice that only the combination of these two methods can document all the channels within the two reference horizons. (d) Simplified illustration of the method used in creating the interpretive plan view maps presented in this study. These maps are composed of successive depth slices and iso-proportional slices. (i) Plan view map of channels generated by iso-propositional slices; (ii) Plan view map of channels generated by depth slice ①; (iii) Plan view map of channels generated by depth slice ②; (iv) Plan view map of channels generated by combining two depth slices and the iso-proportional slice bounded by the top and base of the study area.

Figure 4. Interpreted seismic section and seismic well tie map. **(a)** Interpreted W-E seismic section through the study area. The seismic dataset illustrates the vertical distribution of the eight seismic units and the seven bounding horizons (Top Messinian to Seafloor). Note that Horizon B consists of a unique conformable low amplitude reflection and drapes the paleo incisions, and units SU-2B-I and SU-2B-II are characterised by prominent incisions interpreted as submarine channels. Yellow arrow represents onlap. The gross geometries of the major channel systems are also shown by their “U” or “V” cross-sectional profiles, represented by white dashed lines. **(b)** Seismic-well tie map. Seismic well tie was done to correlate the seismic horizons to their depth equivalent in the borehole. The main study unit SU-2B divided into two subunits. A, B, and C stand for the top, middle and base of the SU-2B unit. Yellow arrows on the log curve show decreasing value of the gamma value, indicating a coarsening upward trend, while the green arrow represents increasing gamma value, implying a fining upward trend. The location of “depth” slice and iso-propositional slices are represented by dashed black and white lines, respectively.

Figure 5. Thickness map of **(a)** unit SU-2B-II and **(b)** unit SU-2B-I, which shows the significant decrease in thickness towards the northeast, indicating a sediment dispersal into the basin in a SW direction. Faults are highlighted in red. Edge in the right side marked with brown triangles represent cutting edge of mass transport deposition.

Figure 6. **(a)** Maximum amplitude map generated 10 m below horizon C (location in Figure 4). Submarine channels and faults are imaged on the map. **(b)** Interpreted variance slice at 1750 m (location in Figure 4) and vertical seismic section (section location in Figure 6a) from the 3D dataset reveal a network of submarine channel features within unit SU-2B-II. Submarine channels are highlighted in blue. The channels here provide useful markers for assessing the strike slip fault systems. Note a meandering channel in the centre, cut and displaced by a SW-NE trending left lateral strike slip fault highlighted by the white dashed line.

Figure 7. Seismic section (location see in Figure 1c) showing the different types of channel in the different levels. Notice that the lower part of each unit is dominated by V-shaped incised channels (c and d) classified as Type-1 channels, while upper part of each unit is dominated by U-shaped incised channels (a and b) and classified as Type-2 channels.

Figure 8. Two interpreted plan-view maps of the submarine channels within the study units. (a) Submarine channels from the lower part (green) and upper part (yellow) of Unit SU-2B-I. Faults are depicted in dark blue. Channels from the lower part have straight to lower sinuosity and an average orientation of N15°W, while channels from the upper part have higher sinuosity and an average orientation of N06°W. (b) Submarine channels from the lower part (green) and upper part (yellow) of Unit SU-2B-II. Faults are depicted in dark blue. Channels from the lower part have straight to lower sinuosity and an average orientation of N02°W degree, while channels from the upper part have higher sinuosity and an average orientation of N06°W degree.

Figure 9. Seismic section showing the characteristics of internal reflection configurations and external forms (left) and its interpretation (right) of different channel-fill styles of the submarine channels identified within the study interval. (a) Convex-upward “hat” filled channel with simple internal geometry; (b) Concave-upward “hat” filled channel; (c) shingled filled channel, in which shingled reflections are dipping towards the last-stage channel incision; (d) Parallel filled channel. The filling reflections consist of moderate-amplitude horizontal reflections; overspill deposits are also delineated. Seismic facies one is typical in Type-1 channel, while the other three seismic facies occur in Type-2 channels.

Figure 10. (a) RMS map of a Type-1 channel in SU-2B-I (location in Figure 8). The channel is filled by relatively high amplitude reflections, and a probable overbank sediments are depicted. Channel is highlighted in red dotted line. (b) Seismic profile crossing the channel shows a convex-upward “hat” shaped filling.

Figure 11. Depth slices (a, c) and seismic sections (b, d) of Type-2 channels (location in Figure 8). Channel **a** shows a flat, parallel filling in cross section. Channel **b** is a meandering channel showing an abandoned channel fill and a last stage channel fill. Channels are highlighted in red dotted lines.

Figure 12. Interpretation of shingled reflection and concave-upward filled channel facies. Depth slice showing a migrating channel facies, (c) Seismic cross section showing the channel filling reflections dipping towards the last-stage channel incision. Channel is highlighted in red dotted lines. (b) RMS amplitude map that shows a meandering channel, showing a low-amplitude in contrast to the surrounding high amplitude strata. (d) Seismic cross section showing the concave-upward geometry of the channel. Channels are highlighted in black dotted lines.

Figure 13. A correlation map of relative sea level, sedimentation rate and seismic cross section of the Post Messinian successions of the Levant Basin. Relative sea level was calculated from oxygen isotopes Miller et al. (2011), sediment discharge of Nile River was calculated from Macgregor (2011). Age estimation of the top Messinian and top Pliocene is based on Schattner et al. (2016).

Figure 14. Conceptual model explaining the evolutionary pattern of submarine channels in light of the interpreted depositional environment. (a) Lower sediment discharge with relatively higher sea level, which resulted in deposition of pelagic to hemipelagic sedimentary unit SU-2A, represented by parallel to subparallel, low amplitude reflections in seismic profiles; (b) High sedimentation rate with relatively sea level falling, which resulted in the development of submarine channels in the lower part of SU-2B-I. Those submarine channels are characterised by V-shaped, low sinuosity and sandy channel incisions; (c) High sedimentation rate with relative sea level rise that resulted in deposition of upper part of SU-2B-I, which was incised by U-shaped, higher sinuosity and muddy channels; (d) High sedimentation rate when relative sea level reached its maximum in this period that resulted in a higher sea level and deposition of hemipelagic sediments characterised by parallel to subparallel, low amplitude reflection B in seismic profiles and without any channel incisions; (e) High sedimentation rate with relative sea level fall, which resulted in the development of submarine channels in the lower part of SU-2B-II. These submarine channels were characterised by V-shaped, low sinuosity, sandy channel incisions; (f) High sedimentation rate with relative sea level rise, resulting in the deposition of the upper part of SU-2B-II, which was incised by U-shaped, higher sinuosity and muddy channels; (g) Decreasing sedimentation rate with relative sea level rise that resulted in the deposition of hemipelagic sediments, characterised as parallel to subparallel, low amplitude

reflections, without channel incisions (unit SU-2C). Note that the stratigraphic layers and sea levels are not to scale.

Table Captions

Table 1: Main types of channel morphologies as observed in the studied interval. The description and the parameters include channel width (CW), channel relief (CR), sinuosity (SI), and width-depth ratio of these types of channel systems.

Table 2: The four major seismic facies and their respective descriptions as identified in the studied interval.

ACCEPTED MANUSCRIPT

Table 1

Units		Number of Channels	Section view description	Plan view parameters				Channel Type
			Incision shape	Average CW (m)	Average CR (m)	CW/CR Ratio	Average SI	
SU-2B-I I	Top	23	U shaped	198	31	6.4	1.11	Type 2
	Base	12	V shaped	120	22	5.5	1.05	Type 1
SU-2B-I	Top	22	U shaped	201	33	6.1	1.13	Type 2
	Base	10	V shape	130	23	5.7	1.04	Type 1

ACCEPTED MANUSCRIPT

Table 2

Channel Type	Seismic facies	Reflection configuration	Internal seismic texture		External geometry
			Amplitude	Continuity	
Type -1	Facie 1	Sub-parallel	Variable	High	Convex-up
Type -2	Facie 2	Sub-parallel	High	High	Concave-up
Type -2	Facie 3	Chaotic	Low	Moderate	Shingled
Type -2	Facie 4	Parallel	Variable	High	Horizontal Parallel

ACCEPTED MANUSCRIPT

Highlights:

- Pliocene submarine channels in the Levant Basin show a duplex-storey architecture
- Two channel types are identified based on morphology and internal architecture
- Channels are driven by an interplay of climate change and sea level fluctuations

ACCEPTED MANUSCRIPT

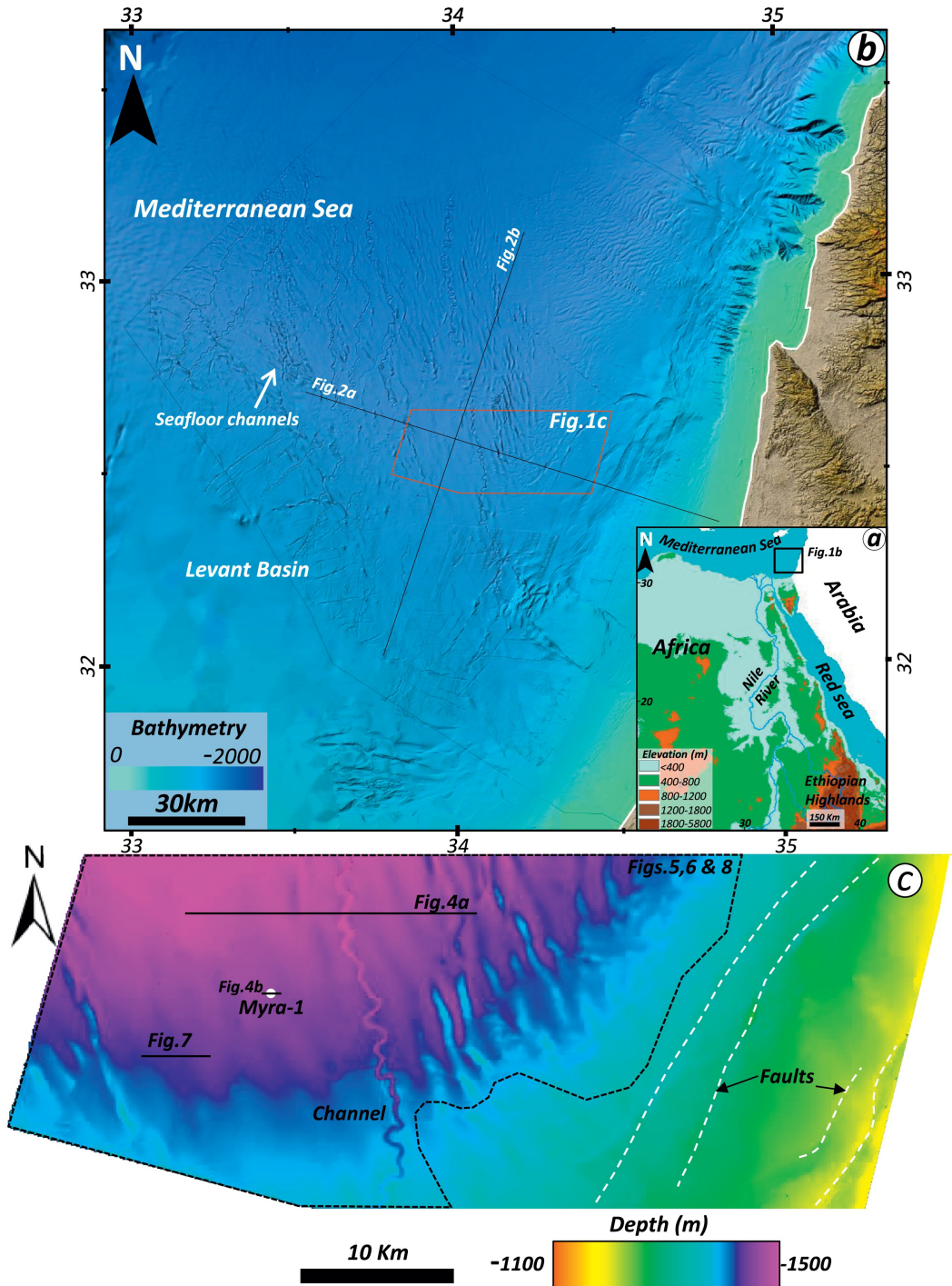


Figure 1

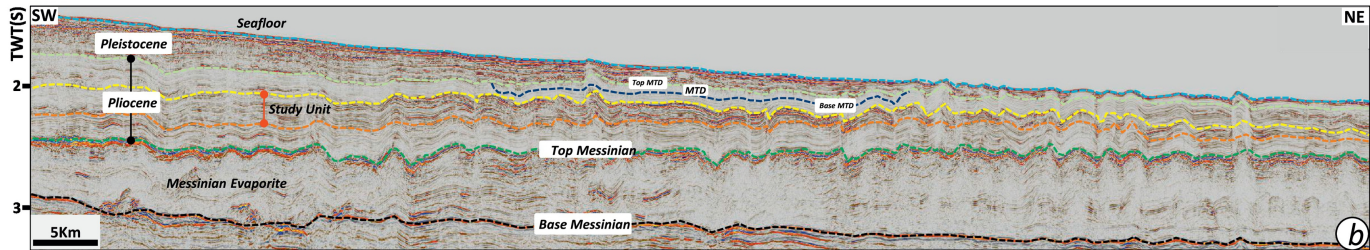
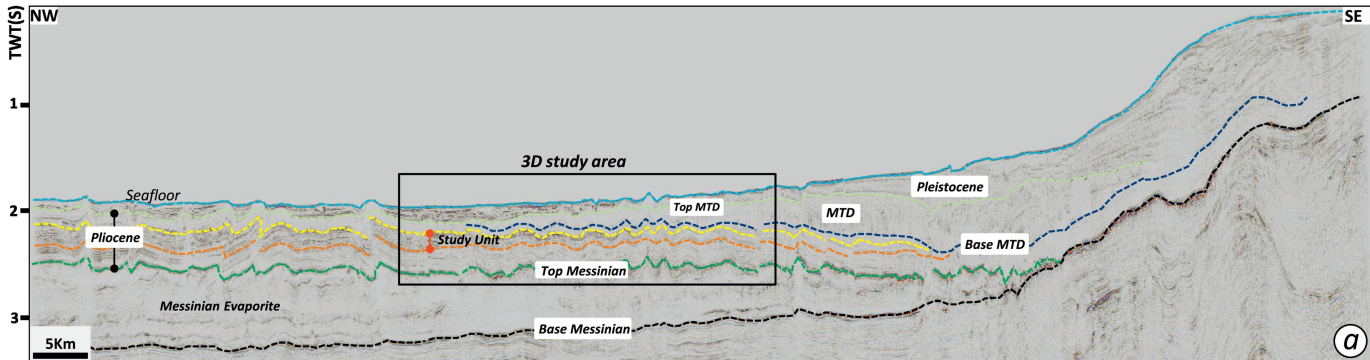


Figure 2

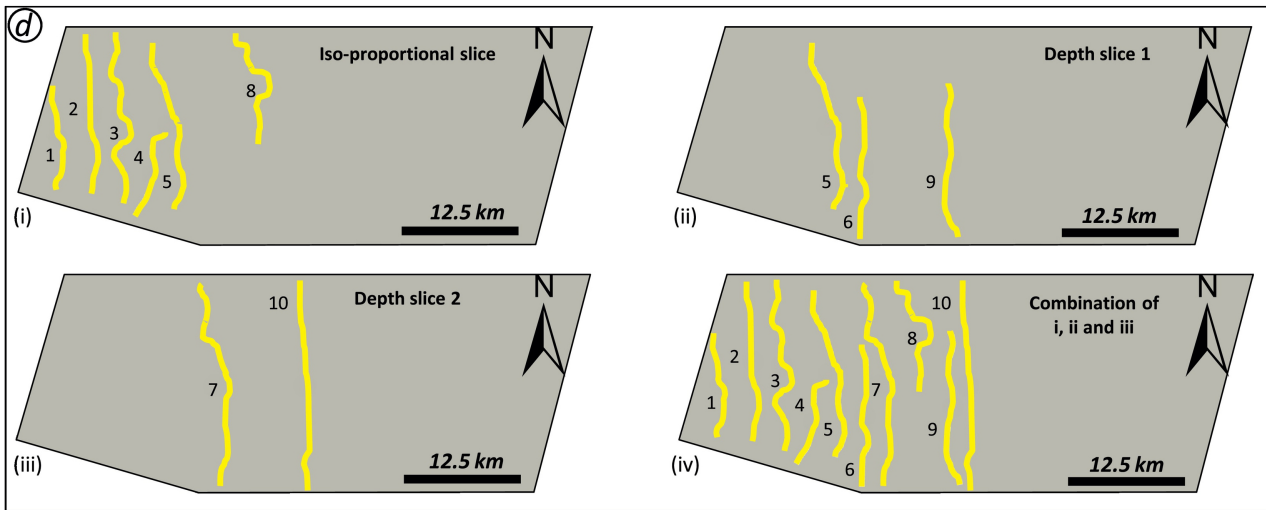
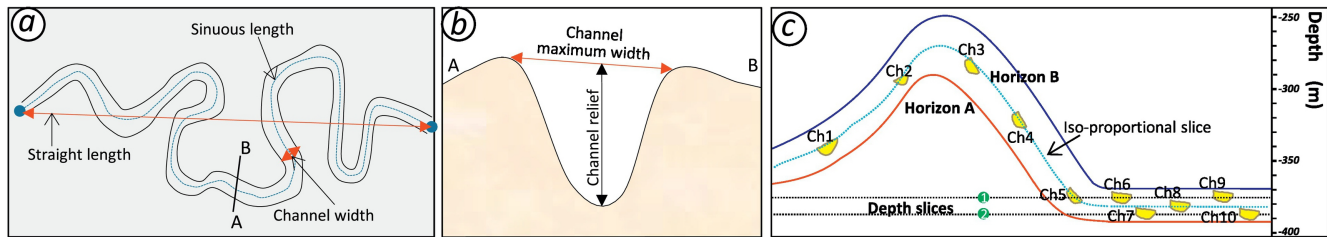


Figure 3

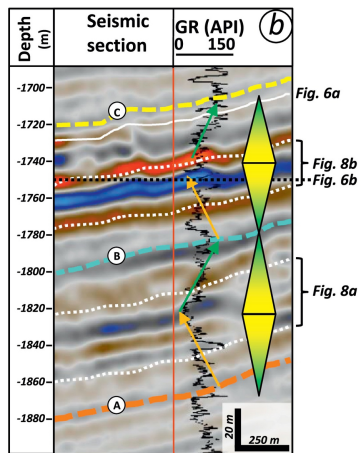
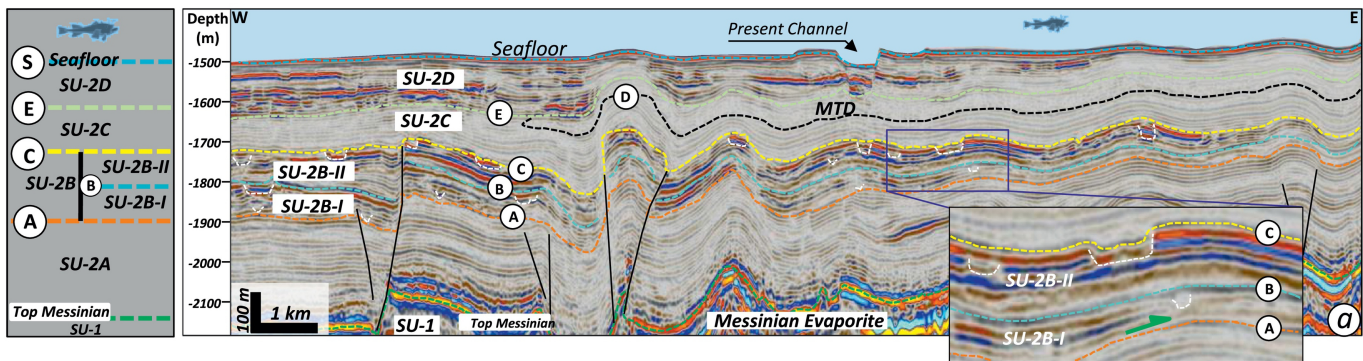


Figure 4

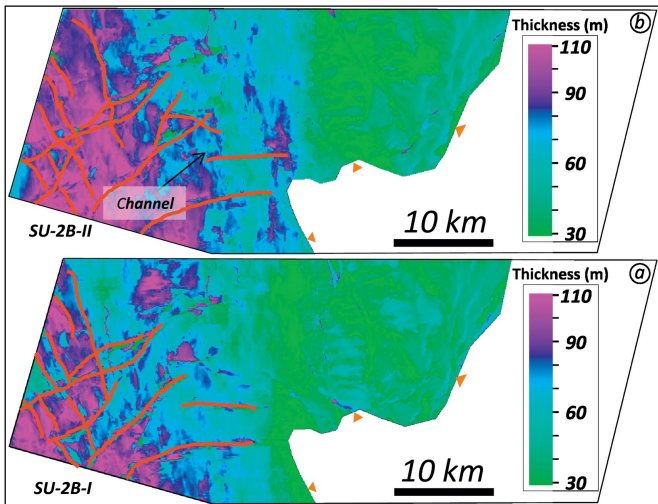


Figure 5

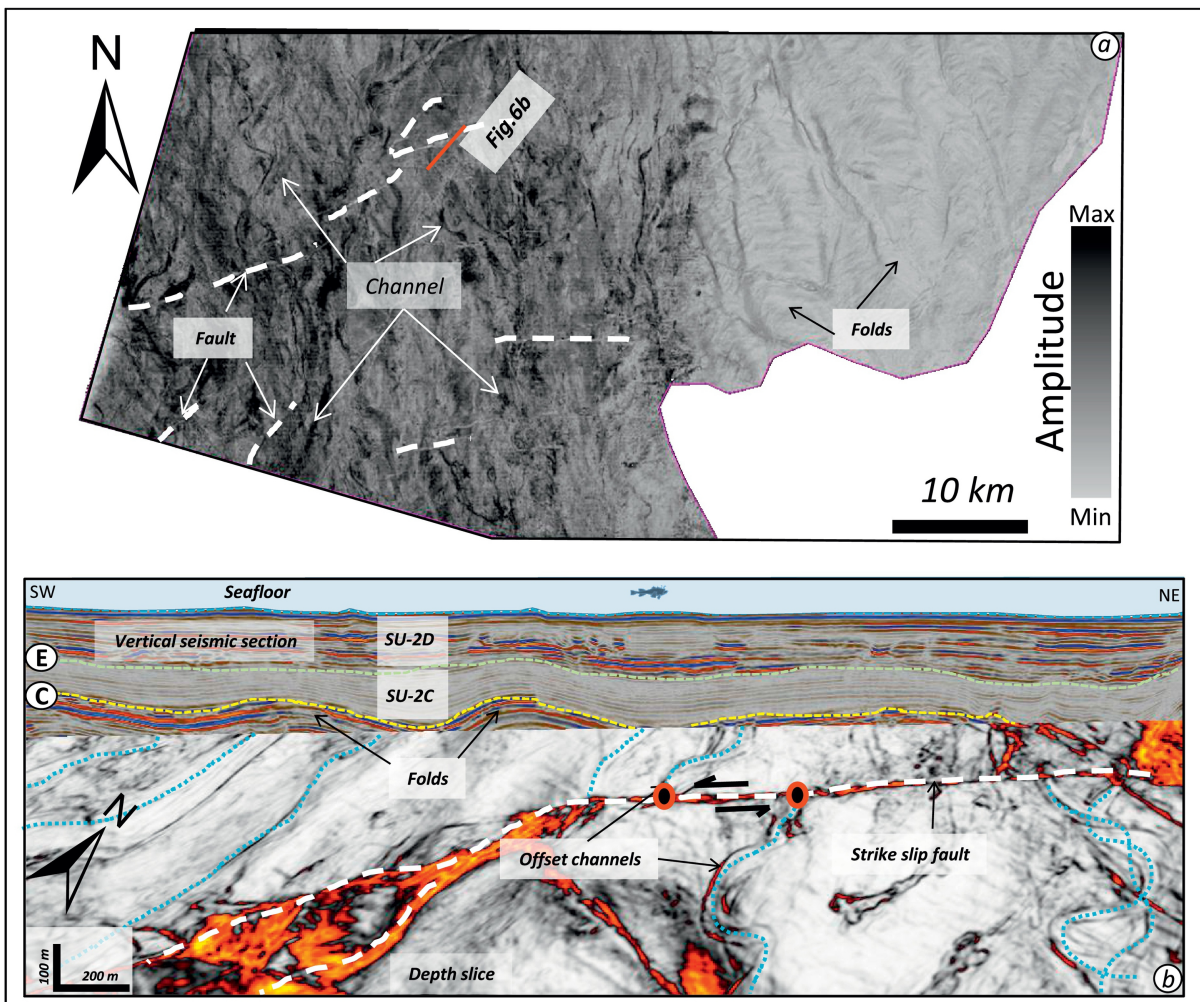


Figure 6

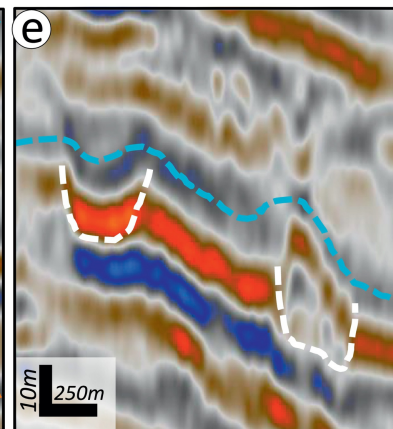
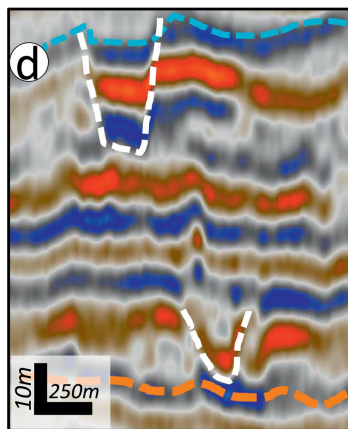
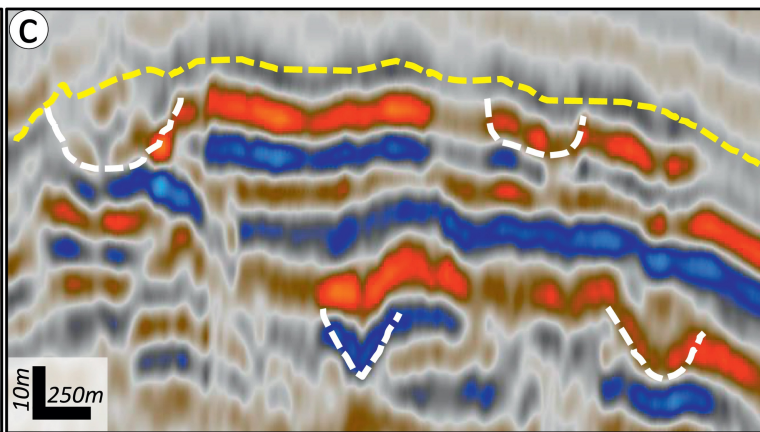
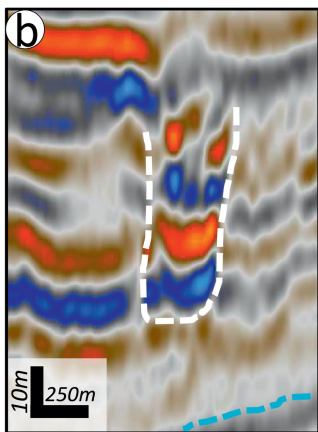
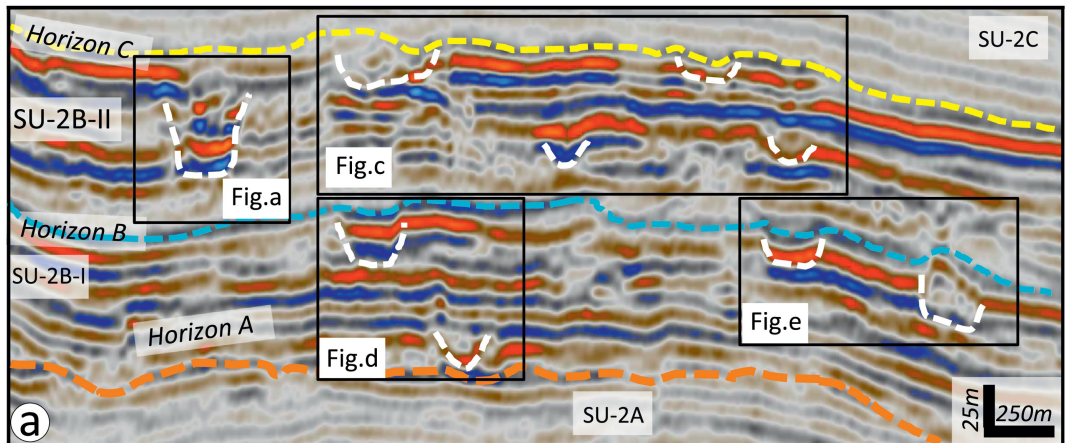


Figure 7

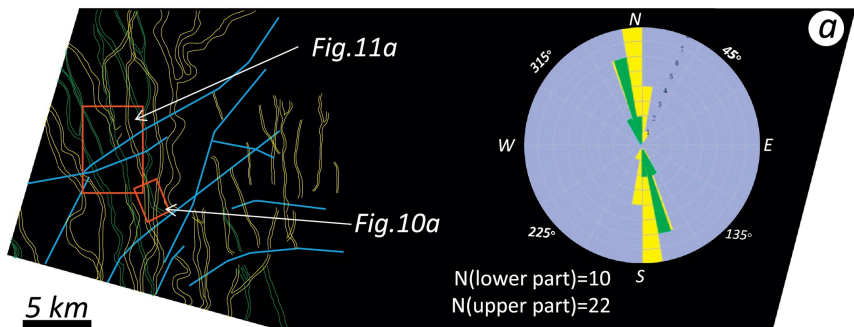
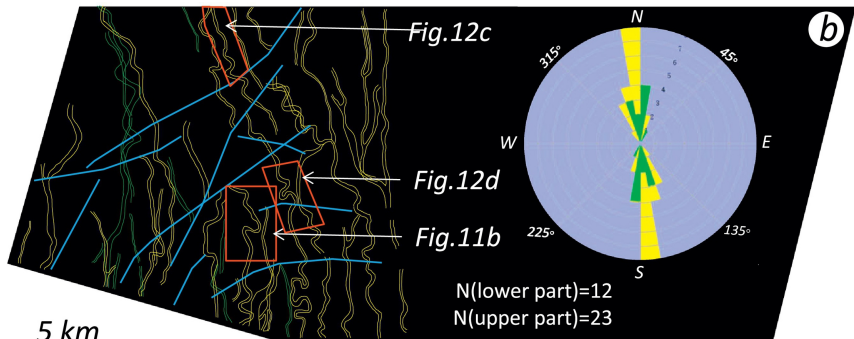


Figure 8

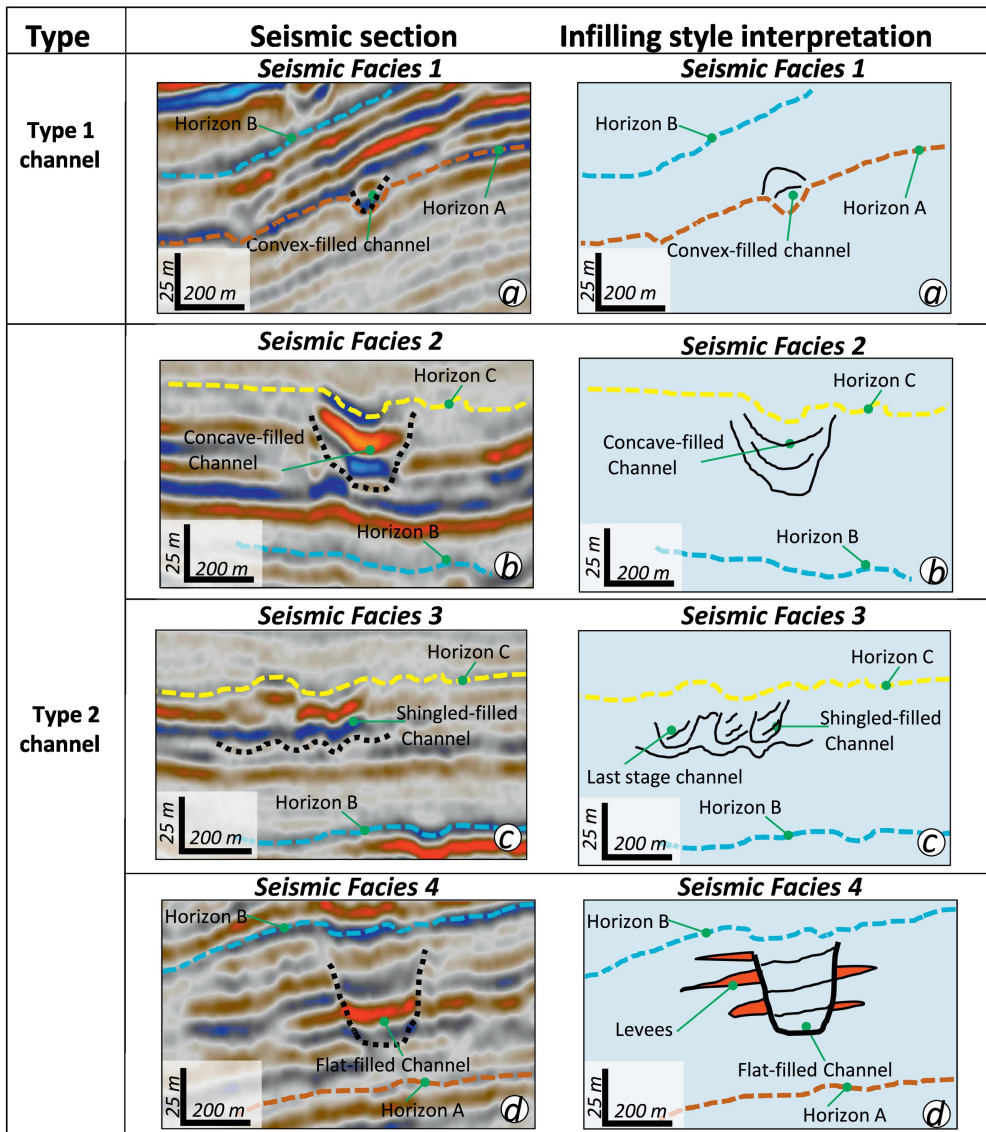


Figure 9

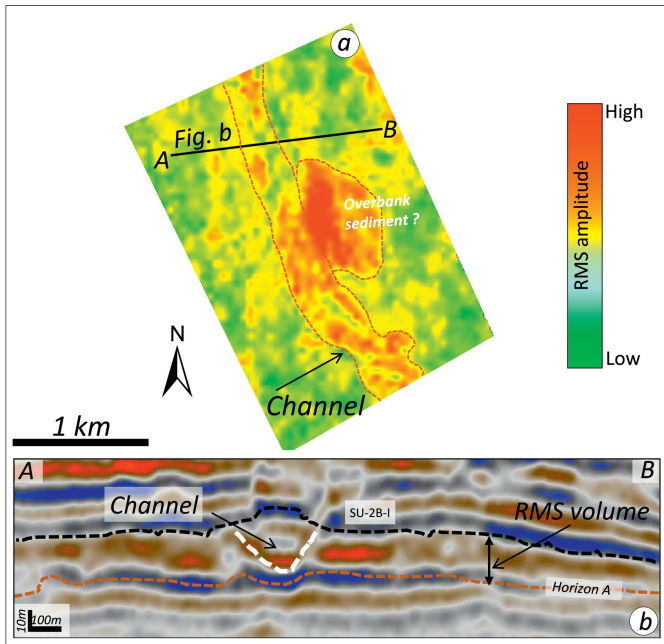


Figure 10

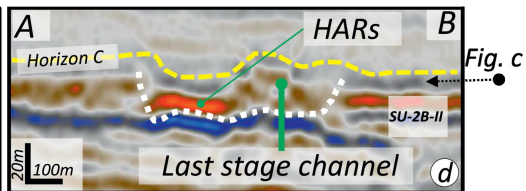
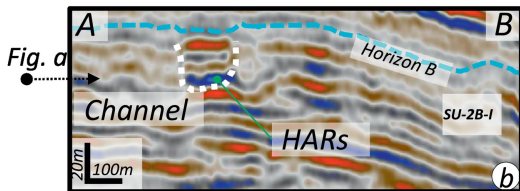
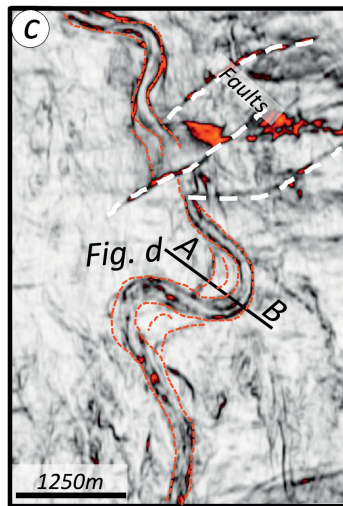
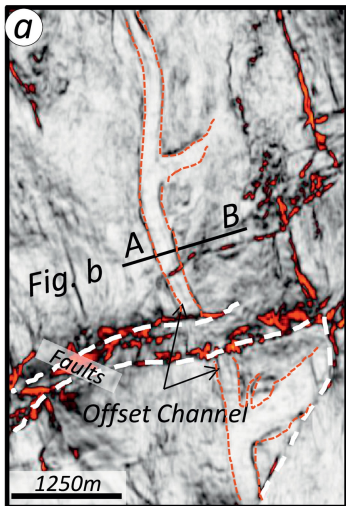


Figure 11

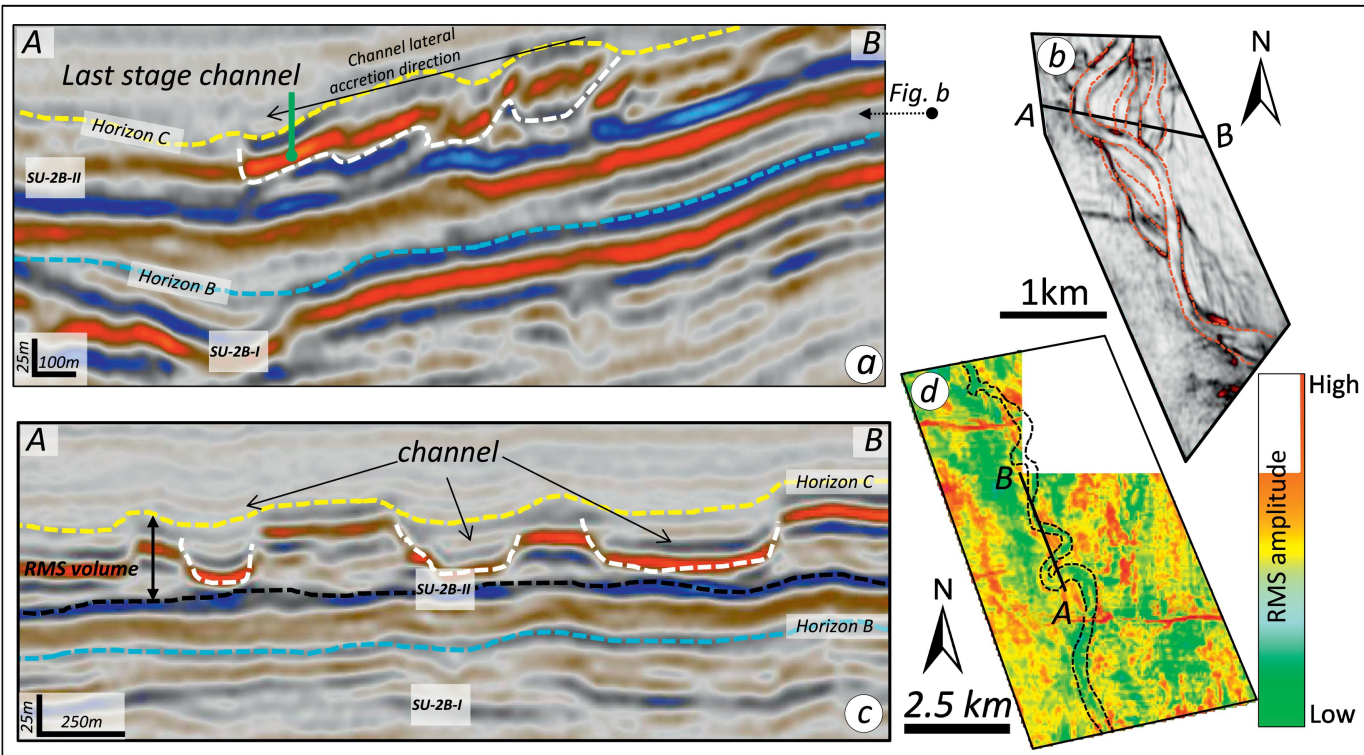


Figure 12

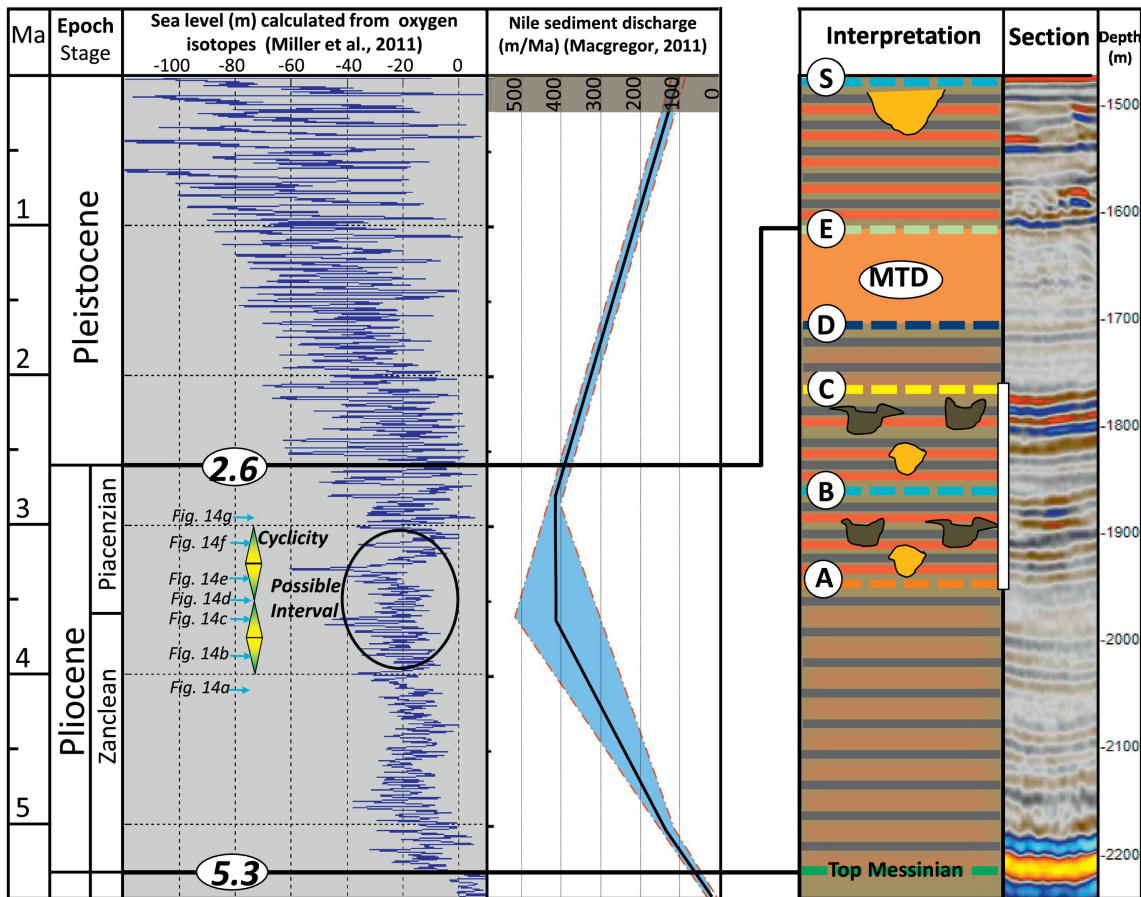


Figure 13

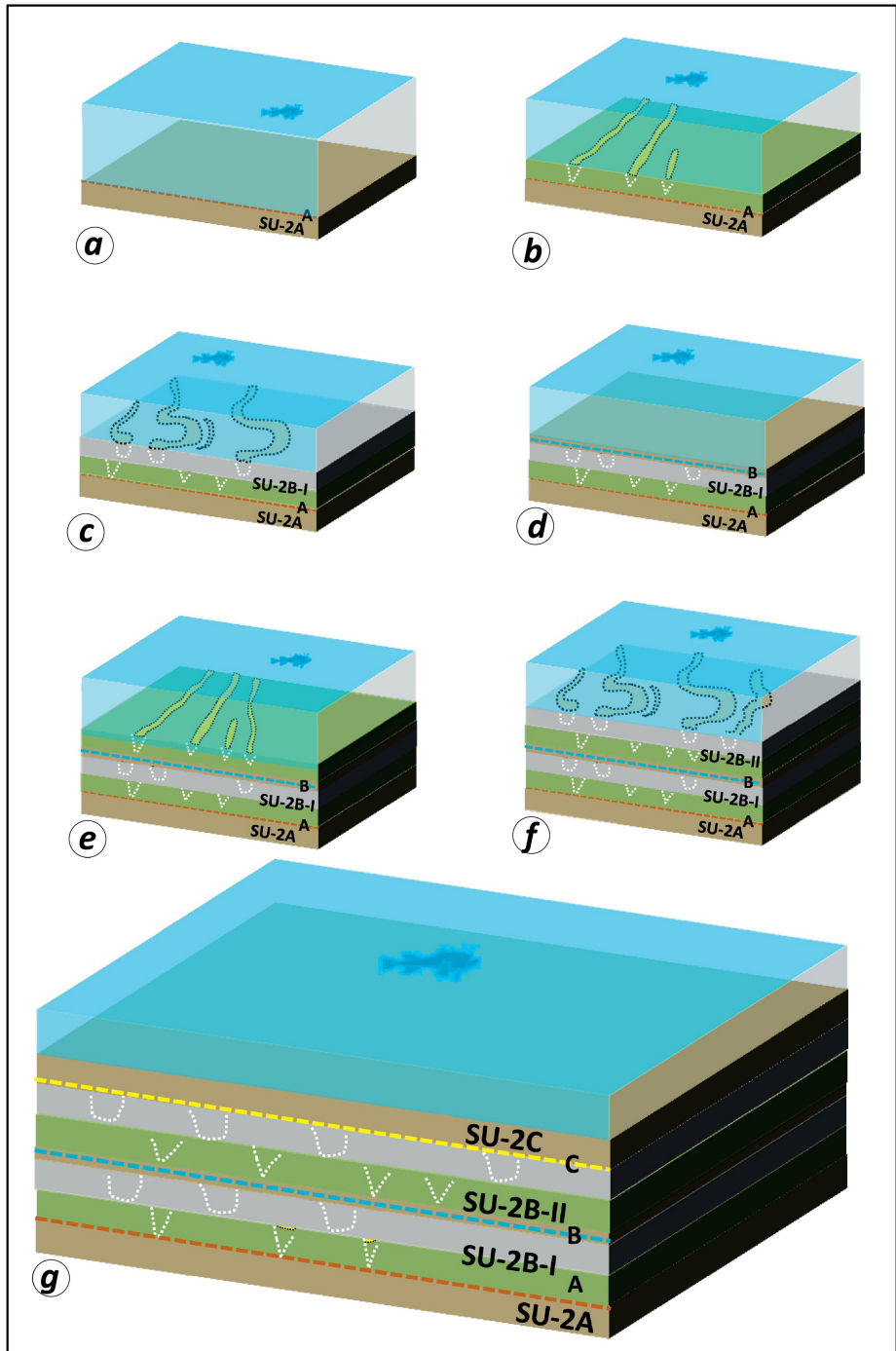


Figure 14